PREPARATION AND CHARACTERISATION OF HIGH ASPECT RATIO MATERIALS FOR BONE TISSUE ENGINEERING

A THESIS SUBMITTED IN PARTIAL FULFILMENT OF THE REQUIREMENT FOR THE DEGREE OF **MASTER OF TECHNOLOGY**

IN

BIOTECHNOLOGY

Submitted by

Alisha Prasad

213BM2034

Under the supervision of

Prof. Sirsendu Sekhar Ray

Department of Biotechnology & Medical Engineering

National Institute of Technology, Rourkela

NATIONAL INSTITUTE OF TECHNOLOGY, ROURKELA

DECLARATION

I hereby state to the best of my knowledge and belief that the project entitled "**PREPARATION AND CHARACTERISATION OF HIGH ASPECT RATIO MATERIALS FOR BONE TISSUE ENGINEERING**" is a record of original work carried out by me under the supervision of **Prof.S.S.Ray**, Dept. of Biotechnology & Medical Engineering, NIT, Rourkela. The results embodied in this project report are solely for academic purpose.

Date: 1.06.2015

Place: Rourkela

Alisha Prasad

ACKNOWLEDGEMENT

I am extremely fortunate to be involved in an exciting and challenging research project entitled "**Preparation and Characterization of High Aspect Ratio Materials for Bone Tissue Engineering**". It has enriched my life, giving me an opportunity to work in a new environment. This project increased my intuition and decipherment capability as I started the project from ground zero level.

While bringing out this thesis to its final form, I came across a number of people whose contributions in various ways have helped me in my field of research and they deserve special thanks. It is a pleasure to convey my gratitude to all of them. First and foremost, I would like to express my deep sense of gratitude and indebtedness to my supervisor **Prof. S.S. Ray** Sir for his invaluable encouragement, suggestions and support from early stage of this research and providing me extraordinary experiences throughout the work. Above all, his priceless and meticulous guidance at each and every phase of work inspired me in innumerable ways. He has triggered and nourished my intellectual maturity that will help me for a long time to come. I am proud to state that I had the wonderful opportunity to work with an eminent Professor like him.

I am highly grateful to **Prof. S.K. Sarangi**, Director, National Institute of Technology, Rourkela and **Prof. K. Pramanik**, H.O.D., Biotechnology and Medical Engineering for their kind support and permission to use the facilities available in the Institute. I owe a debt of gratitude to **Prof. Mukesh Gupta** and Erasmus Mundus for giving me the opportunity to visit Uppsala University as an exchange student and carrying out research there and giving me an international exposure. I also thank **Dr. Ken Welch** and **Dr. Maria Stromme** for allowing me to conduct research in their lab, at Angstronglabrotoritet and their continuous guidance and support. I express my thankfulness to my lab mates- **Narendra, Joseph, Rik** and **Priyanka** for their continuous encouragement, suggestions and competition. I am obliged to my juniors- **Abinaya** and seniors **Abhijeet Barua** and **Bhishm Singh** for the constant talks and suggestions.

I am deeply indebted to my family members and dedicate my thesis to Papa and Maa, and hope someday soon I become like you following your footsteps. Thank, you for all the moral support, continuous encouragement and love.

Alisha Prasad

NATIONAL INSTITUTE OF TECHNOLOGY, ROURKELA

DEPARTMENT OF BIOTECHNOLOGY AND MEDICAL ENGINEERING

CERTIFICATE

This is to certify that the thesis entitled **"PREPARATION AND CHARACTERISATION OF HIGH ASPECT RATIO MATERIALS FOR BONE TISSUE ENGINEERING"** submitted by Ms. ALISHA PRASAD in partial fulfillment of the requirements for the award of the degree of Master of Technology in Biotechnology at the National Institute of Technology, Rourkela is an authentic work carried out by her under my supervision and guidance.

To the best of my knowledge, the matter embodied in the thesis has not been submitted to any other University/ Institute for the award of any Degree or Diploma.

Date: 01.06.2015

Dr. S.S. Ray

Assistant Professor

Department of Biotechnology and Medical Engineering

National Institute of Technology Rourkela

CONTENTS

List of Tables

List of Figures

List of Graphs

ABSTRACT

This research work aims to give an overview of the synthesis of high aspect ratio materials for bone tissue engineering. The work was carried out using high aspect materials of both natural (micro fibrillated cellulose from jute, spider silk, cocoon silk) and synthetic grade (MgO and ZnO nanorods). Micro fibrillated cellulose was extracted from jute by washing it thoroughly with sodium hydroxide and bleaching it with hydrogen peroxide followed by acid hydrolysis with sulphuric acid. Spidroin was extracted from spider silk using different benign solvents and fibroin was extracted from *Bombyx mori* following the lithium bromide standard protocol. Hydrothermal method was followed for synthesis of magnesium oxide and zinc oxide nanorods. Micro fibrillated cellulose was characterized by SEM, XRD, FTIR, DSC, TGA, dispersion studies, and phytochemical tests. Spidroin and fibroin was analyzed using Fluorescence microscopy, FTIR, and CD. Magnesium oxide and zinc oxide nanorods were characterized using SEM, and XRD. Also, a comparative *in-vitro* cytotoxicity of all these materials was checked using adipose derived stem cells (ADSCs). From the SEM results it was found that the cellulose extracted from jute were micro fibrillated. The FTIR and XRD data showed that cellulose type II was extracted. Also the degradation of cellulose at 270 °C was confirmed from TGA results. Both spidroin and fibroin was successfully extracted using simple benign solvents. FTIR and CD data showed the presence of good amount of β-sheets. FESEM of both MgO and ZnO showed that the nanoparticles agglomerated together to form nanorod like structure. The MTT study revealed that spider silk was more compatible followed by cocoon silk, cellulose, MgO and ZnO. This concludes that while both the high aspect ratio as well as the biocompatibility of the materials is an important factor designing materials for load bearing application.

Keywords: Cellulose, Spider silk, Cocoon, MgO, ZnO, high aspect ratio

INTRODUCTION

1.1.Introduction

Bone is a complex, dynamic and highly vascularized connective tissue providing structural support to the body. Bone is a mineral reservoir supporting muscular contractions leading to movements of different parts of the body, load bearing capacity and protecting internal organs of the body[1]. Its characteristic property to heal and remodel itself during injury without leaving a scar by utilizing its mineral stores makes it the ultimate smart material. Any alterations in the bone structure due to injury/disease can drastically alter the body's equilibrium and affect the quality of life[2]. Research shows that though bone regenerative medicine has achieved progress in years, current therapies, such as bone grafts, still have several limitations as most of the severe bone injuries are still unrecoverable and not adequately treated[3].

Introduction of bone tissue engineering involving design of engineered bone tissue via combination of biomaterials from various sources, cells, and factor therapy as a substitute to bone grafts has shown potential advancement in this field, due its limitless supply and no disease transmission[4]. Merging of tissue engineering and regeneration has provided a platform for new dimensional medical research[5]. This includes design of biomimetic, biocompatible, biodegradable scaffolds along with the coordination of cells and biologically active signaling molecules to improvise the existing bone models in relation to mechanical strength, compatibility, ease of access and immune-rejection[6].

Bones are connective tissue composed of two main components: a. an organic protein collagen contributing the maximum composition along with, b. an inorganic mineral called hydroxyapatite, which combines to provide mechanical-cum-supportive role in the body[7].

This inorganic mineral, Hydroxyapatite (HA) is the most used materials for bone reconstruction because of its close similarity in composition to human bone and teeth[8] . Thus most research is concentrated around synthesizing different formulations of HA with higher mechanical strength and better osteinductive property[9].

Table 1: List of high aspect ratio materials[10]

Sl no	Material	Elastic Modulus (GPa)
1	Carbon nanotubes	300
2	Stainless steel	200
3	Spider viscid silk	270
4	Magnesium oxide nanotubes	200
5	Zinc oxide nanotubes	250
6	Micro fibrillated cellulose	150
7	Hydroxyapatite(Bone mineral)	80--120
8	Cortical Bone(longitudinal)	11-21
9	Mulberry silk (Bombyx Mori)	16
10	Collagen dry	6

In this study, all the high strength, easily and abundantly available advanced materials have been synthesized, characterized and studied for use as an additive along with HA for better load bearing applications. For this study, high strength materials from both natural and synthetic sources have been extracted and studied. In our study, extraction of materials from natural source material like Jute, Spider Silk, Mulberry Silk (*Bombyx mori*) and synthesis of materials like Carbon nanotubes (CNTs), Magnesium oxide nanorods (MgO) and Zinc oxide nanotubes (ZnO) have been done. The work involved extraction of cellulose from jute, proteins from silk which are listed among the high strength materials for load bearing application in tissue engineering. Apart from these, synthetic materials like carbon nanotubes were also fabricated via one-step pyrolysis to get a synthetic material with a multiple features like high mechanical strength, good electrical conductivity for better osteogenesis, and its characteristic shape opening new dimensions of research for improved drug deliver/ ion-transport inducing better bone healing[11].

Also, advancement of materials science has opened new frontiers in the field of bone tissue engineering involving different compatible materials for use in medical research. With this

prospective, we also fabricated materials like magnesium oxide nanotubes and zinc oxide nanotubes via hydrothermal method to study its compatibility for load bearing applications of bone tissue engineering[12].Instead, this foreword will examine some of the most recent advances in bone tissue engineering and regeneration, emphasizing the interconnected fields of biomaterials, material science, cell biology, signaling biology, and biomaterial research[13].

1.2 AIM AND OBJECTIVE:

To synthesize and characterize materials with high aspect ratio for load bearing applications in bone tissue engineering .

1. To synthesize both natural materials (jute, spider silk and cocoon silk) and synthetic materials (magnesium and zinc oxide nanorods) from readily available sources for serving as the start material.
2. To make comparative study of each material in relation to mechanical strength and in-vitro cytotoxicity with adipose derived stem cells.

REVIEW OF LITERATURE

Steven Spoljaric et.al,Stable, self-healing hydrogels from nano fibrillated cellulose, poly(vinyl alcohol) and borax via reversible crosslinking, European Polymer Journal, 56 (2014) 105–117

Nano fibrillated cellulose was used to enhance the swelling and mechanical properties of the PVA-borax –NFC hydrogel that was formulated. The addition of NFC to the hydrogel was found to reduce the creep and it had a significant impact on the rheological properties of the hydrogel. Also, it was observed that the addition of nfc beyond a particular concentration lead to structural destabilization of the hydrogel as it prevented crosslinking in the fundamental structure of the hydrogel.

Nathalie Lavoineet.al, Micro fibrillated cellulose – Its barrier properties and applications in cellulosic materials: A review, Carbohydrate Polymers 90 (2012) 735– 764

Cellulose occurs naturally as different isoforms out of which the semi crystalline form i.e cellulose I is considered to be the main contributor to the formation of nanocellulosic structures such as nanofibers(5nm),nanocrystals and micro fibrillated cellulose.(20-50nm).the two major sources of nanocellulosic are plants and bacteria. The most common methods to obtain nanocellulosic from plant materials is by acid hydrolysis and the resulting nanocellulosic structures are usually characterized using various techniques such as TEM,SEM,XRD ,AFM mechanical and rheological tests. On the other hand the micro fibrillated cellulose is mainly synthesized using mechanical methods and its barrier properties have led to its use in various applications such as oxygen and water permeability, packaging and printing applications.

Sabrina Belbekhoucheet.alhave also worked on the barrier properties of CNC and MFC synthesized from sisal fibers.

Jinyou Linet.al. Cellulose nano fibrils aerogels generated from jute fibres, Carbohydrate Polymers 109 (2014) 35–43

Cellulose nanofibers have been synthesized using jute as the source and the effects of various pretreatment methods such as usage of NaOH and DMSO to remove non-cellulosic impurities

have been studied usingSAXS and WAXS. The nano fibrils of diameter 5-20nm were generated using TEMPO mediated oxidation methods and characterized using TEM followed by which an aerogel of the nanofibres was prepared using lyophilisation.this aerogel was further charecterised using SEM and WAXS.

Rasha M. Sheltamiet.al, Extraction of cellulose nanocrystals from mengkuang leaves (Pandanus tectorius), Carbohydrate Polymers 88 (2012) 772– 779

The synthesis of cellulose nanocrystals from menkuang leaves has been described and it involved pretreatment with NaOH and bleach for removal of lignin followed by an acid hydrolysis procedure that lead to formation of crystals of size 5-20nm and these crystals were further characterized using techniques such as FTIR to confirm the eradication of lignin,FE-SEM,TEM to determine the size, XRD, to determine crystallinity index of cellulose which was found to be around 69% and TGA to study the thermal characteristics at every stage of synthesis.

Faten Al-Hazmiet.al, A new large – Scale synthesis of magnesium oxide nanowires: Structural and antibacterial properties, Super lattices and Microstructures 52 (2012) 200–209

Magnesium oxide nanowires have been synthesized using hydrothermal oven method and have resulted in rods of diameter of approximately 6nm.The nanowires were characterized using FTIR,XRD,SEM,EDS.The synthesizednanowires were also found to bacteriostatic activity against gram negative and gram positive bacteria.

Hao Zhang et.al, Preparation and characterization of silk fibroin as a biomaterial with potential for drug delivery Journal of Translational Medicine 2012, 10:117

They have made a comparative analysis of fibroin in various solutions. Degumming is done to remove sericin which is a sticky coating on the fibroin SDS PAGE analysis gives us an estimate of the molecular weights of the fibroin protein. The outcome was as follows (in the ascending order):-

$Ca(NO_3)$-MeOH, Ca (NO_3)-EtOH, $CaCl_2$-MeOH, $CaCl_2$-EtOH.

Thus we can very easily deduce that the CaCl2-EtOH preserved the secondary bonds and did not lead to bond-cleavage and thus the fibroin was not broken into smaller units. Therefore, it showed

the highest molecular wt. and was even characterized by the absence of any lower MW units. Degummed silk did not show any bands at all; thereby corroborating to the fact that fibroin is not soluble in degummed silk solution (devoid of any specific solvent). According to the data obtained from FTIR it was inferred that the fibroin is essentially composed of alpha helices, beta sheets and a region of random coils as well. CaCl2-EtoH gave more amount of Silk II (alpha form, type II beta turn) while the remaining three gave more amount of Silk II (beta form, anti-parallel beta pleated sheets). Hence this again testifies to the fact that CaCl2-EtOH solution preserves the native Silk I form of fibroin.

WAXD, the fourth analysis step. This was carried out in order to determine the crystalline structure of the regenerated silk fibroins from the four solutions. The results are as follows:-

Degummed fibroin and Ca (NO_3)-MeOH, $CaNO_3$-EtOH and $CaCl_2$-MeOH rendered peaks corresponding to both Silk I and Silk II types, whereas $CaCl_2$-EtOH gave peaks corresponding to the Silk I type only. Thus, $CaCl_2$-EtOH increases the crystallization ability of fibroin but the rest three causes attenuation in the crystallization ability of fibroin. Also, again, CaCl2-EtOH retains the native form of fibroin.

The obtained fibroin was then used to determine alterations in the activity of a specific enzyme after it bio conjugated with the fibroin solutions

J. M. Goslineet.al. The mechanical design of spider silks: from fibroin sequence to Mechanical function, The Journal of Experimental Biology 202, 3295–3303 (1999)

The silk isolated from different species of spider have been compared. Spider silk has proven to have high mechanical strength in comparison with other engineering materials and these mechanical properties are seen to vary with temperature and moisture content. The main secondary structure present in the spidroin protein is the beta pleated sheets and the alternative arrangements of the amino acids glycine serine and alanine are responsible for the formation of such structures. Spider silk could thus serve as an excellent protein based structural biomaterial.

Chapter 1

SYNTHESIS AND CHARACTERISATION OF MICROFIBRILIATED CELLULOSE FROM JUTE

1.1. Cellulose is the most abundant natural, degradable, renewable material available in nature in from various sources like wood, pulp, straw, cotton, plant stems etc.[14]. Cellulose is a naturally occurring polysaccharide obtained via series of extraction from natural sources and hence can be used in various medical applications, due to its inherent characteristics like excellent mechanical strength, non-toxicity, insolubility with water, stability in different pH and temperature conditions[15]. The structure of cellulose is made up of a long linear homo-polysaccharide chain composed of β-D-glucopyranose units linked together by β-1-4-linkages[16]. Each monomer in the cellulose structure contains three OH-groups (hydroxyl), which helps in formation of hydrogen bonds imparting different structural entity depending on the bond formation and packing like, micro fibrillated cellulose, micro fibrils or crystalline cellulose[17].

1.2.Structure of cellulose:

Cellulose is considered a green –world material not only from its abundance and renewability, but because of the high mechanical strength and stiffness it offers similar to the cortical bone[18]. Also it is, hydrophilic, biocompatible, and it can be easily modified to introduce new functional groups as per utility[19]. The most abundant and readily available source of cellulose is wood, which consists of a network of cellulose fibers entrapped within a matrix of lignin and other natural polymers like hemicellulose which can be easily degraded and removed to isolate cellulose[20]. The process adapted for isolation of cellulose results in different forms of cellulose like micro fibrillated, micro fibrils, nano-fibrillated cellulose, nano- crystalline cellulose and nano cellulose-whiskers[21].

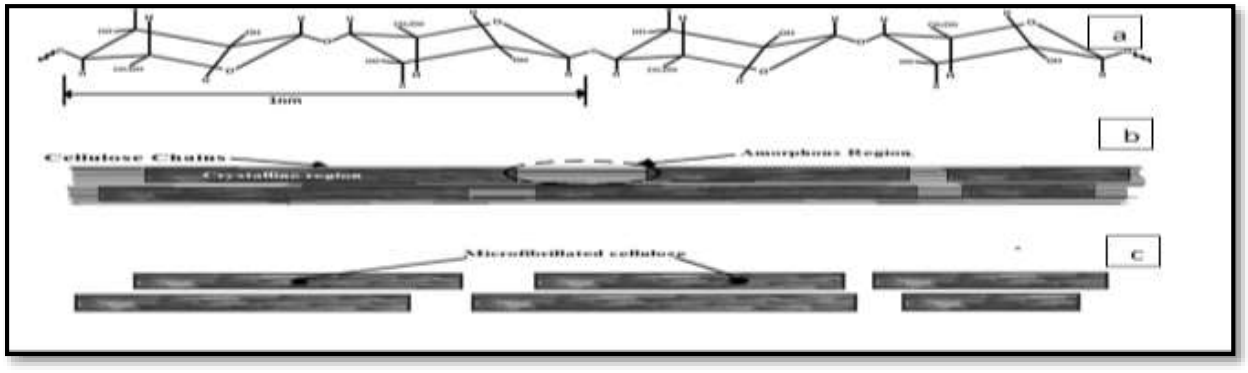

Figure 1: Principle of Cellulose isolation a. linear polysaccharide chain, b. before acid hydrolysis and c. after acid hydrolysis

1.3.Isolation of cellulose:

Cellulose isolation requires a series of steps to break open the trapped cellulose this is discussed below:

1. The staring material that is wood or pulp has to be chopped into fine pieces prior to treatment. Smaller in size the starting material, more would be the surface area for treatment, better would be the isolated form of cellulose obtained in relation to size[22].
2. Initially the chopped fibers/pulp is dewaxed, de-lignified to remove the oily, greasy waxy materials present in it.
3. After this the material is washed using caustic soda and bleached prior to acid hydrolysis to remove any unwanted lignin.
4. MFCs are material that neither is soluble in water, nor does it depolymerize[23]. The ether bonds linking the glucose units of the cellulose cannot be easily broken apart, and requires strong acid treatment to enable cleavage reactions. There are different protocols followed to enable cleavage reactions like acid treatment via sulphuric acid, hydrochloric acid or by using strong oxidizing agents like TEMPO[24].
5. The strong hydrogen bonds between cellulose molecules makes it tough to break open and hence requires treatment at high temperature under a closed chamber with a sufficient amount of surface area for the amorphous regions of cellulose to break open in order to form MFCs. In order to form crystalline cellulose the material has to be treated at 320° C and 250 pressures to allow enough water to intercalate between the cellulose molecules to cause them to become amorphous in structure[25].

1.4.Advantage of Micro fibrillated cellulose:

In comparison with nano crystalline cellulose: Cellulose exhibits certain interesting features due to the presence of hydroxyl (OH) –bonds which can form hydrogen bonds along with water molecules making cellulose hydrophilic[26]. Because of the small size of the nano-cellulose ,both the cellulose obtained from the supernatant and the residue can engorge water forming H-bonds and swelling to nearly double its actual dry weight due to occurrence of nano-defects. This nano-

defect is quite minimal but is not seen in case of micro fibrillated cellulose due to its large size as comparison to the later[27].

1.5.In comparison with other strong reinforcing materials:

Carbon nanotubes (CNTs) and Spider Silk are the only two materials which have a stronger reinforcement than micro fibrillated cellulose[28]. The disadvantage of CNTs is their high cost and of spider silk is that the material isolation is tedious. On the other hand, micro fibrillated cellulose is cheap and can be readily isolated in large quantities.

1.6.Jute as source for MFC:

Jute (*Chorchorus capsularis*) is the most abundant source of biodegradable and recyclable natural fiber in the world just after cotton[29]. It is primarily composed of cellulose and lignin and is brownish in color. There are many varieties of jute found in India mainly in the eastern part of India bordering Bangladesh. *Chorchorus capsularis* and *Chorchorus olitorius* are the most cultivated jute fibers found. Earlier, jute was used extensively for packaging and industries but due to globalization jute has lost its utility despite of its excellent properties and hence its utility can be much more focused as a source for MFC.

2.1.MATERIALS AND METHODS

2.1.1. Materials:

Jute, was purchased from Karimganj, Silchar, Assam, India, Sodium Hydroxide (NaOH), Hydrogen Peroxide (98% pure), Sulphuric acid (98% pure),Fetal Bovine Serum, Antibiotic-Antimycotic solution, MTT assay kit and Nutrient Broth were purchased from Himedia, Mumbai, India, Zinc Nitrate Hexahydrate, Ammonia (98% pure), Magnesium hexahydrate , Urea was purchased from S.D.Fine – Chem. Ltd.*Bombyx mori* was purchased from. The ADSC was procured from NCCS, Pune. All other chemicals used were of analytical grade and were obtained locally.

2.1.2. Methods:

2.1.2. a Pre-treatment of Jute fibers:

The raw jute fibers were first chopped into small pieces of nearly 1-2 cm fiber size and was kept soaked in distilled water for removal of dust and dried at 80 °C until dry prior to use[30]. After this to remove the non-cellulosic constituents like wax, lignin the washed and dried jute fibers were first de-lipidized using toluene/ethanol (2:1 v/v) ratio as solvent in a Soxhlet apparatus for 6-8 hrs. After removal of the lipids, the fibers were washed thoroughly in running distilled water to remove any solvent if present. Subsequently, the treatment process for cellulose isolation was then followed. The fibers, where then soaked in NaOH (30 % w/v) overnight under stirring condition in a closed bottle maintaining temperature at 80 C[31]. Again the fibers were re-washed in running distilled water to wash out excess NaOH after which the drenched fibers were bleached with hydrogen peroxide (30 % v/v) until the appearance of brown- fibers to yellowish- fibers (approximately 10-12 hrs). The pH of the system was maintained using acetic acid.

2.1.2. b Micro fibrillated cellulose production

The pre-treated dried mass collected, was hydrolyzed in concentrated sulphuric acid (60 % v/v) for 10-12 hrs. at 80° C[32]. After acid, hydrolysis, the sample was neutralized with NaOH (10 % wt/v) by slowing adding the pellets. The neutralized samples were then centrifuged with distilled at 6000 rpm for 10 mins until removal of brown supernatant. Both the supernatant and the residue

were then dialyzed until neutral pH. After this the residue was dried in an oven at 60° C for 24 hrs and the supernatant was kept aside for further characterization and study. (10)

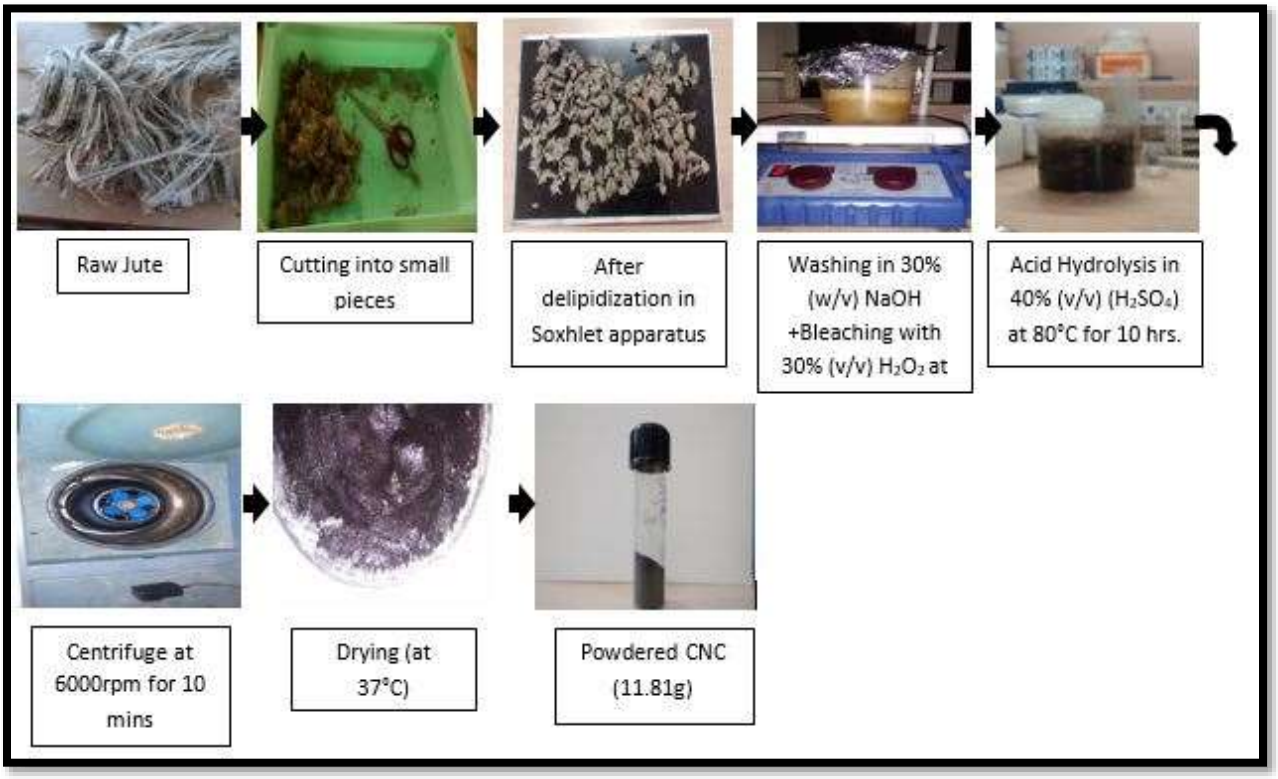

Figure2: Extraction procedure of micro fibrillated cellulose from jute

3.1. CHARACTERIZATIONS OF MICRO FIBRILLATED CELLULOSE:

3.1.1. Shape and morphology

The samples were examined under an optical microscope at each stage of synthesis. The shape and surface morphology of the dried powdered residue was determined by using scanning electron microscope (JEOL-JSM 6480, Japan) after coating with a thin layer of platinum (Pt). SEM images were used to measure the length of the fibrils.

3.1.2. Phytochemical Tests (11)

After delignification, of the jute fibers in a Soxhlet apparatus, the delignified solvent was tested to check the different phytochemical present in the extract.

The following list of tests was carried out:

1. **Test for Tannins:** For checking the presence of tannins, 1ml of jute extract, was mixed with 2 ml of 5 % ferric chloride. The formation of a dark blue/greenish-blue color confirms the tannin test positive[33].
2. **Test for alkaloids:** For alkaloids test, 2 ml of jute extract was mixed with 2 ml of Wagner's reagent. Reddish brown color precipitate confirms the alkaloids test positive[34].
3. **Test for flavonoids:** For flavonoids, 2ml of jute extract was added to 2N sodium hydroxide. Appearance of yellow color confirms flavonoids test positive.
4. **Test for terpenoids:** For terpenoids, 0.5 ml of jute extract was mixed with 2 ml of chloroform. To this mixture, few drops of concentrated hydrochloric acid were added slowly along the sides of the testube. Formation of a red brown color at the interface confirms the terpenoids test positive.
5. **Test for saponins:** For saponins, 2 ml of jute extract was mixed with 2 ml of distilled water and vortexed for 5-10 minutes. Formation of a 1 cm foam layer confirms the saponins test positive.
6. **Test for quinines:** For quinines test, 1 ml of jute extract was mixed with 1ml of concentrated sulphuric acid. Appearance of red color confirms the quinines test positive.
7. **Test for steroids:** For steroids, again 1 ml of jute extract was mixed with 1 ml of chloroform. To this mixture, few drops of concentrated hydrochloric acid were added

slowly along the sides of the testube. The formation of a brown ring at the interface confirms steroids test positive[35].

3.1.3. Dispersion studies

The micro fibrillated cellulose nanocrystals prepared, were dispersed in different organic solvents to study its dispersing characteristics as well as its interaction. 1 g of the dried micro fibrillated cellulose, were dispersed in 10 ml of different solvents like methanol, acetonitrile, DMSO, DMF, chloroform and toluene to study it in various suspensions. These suspensions were sonicated using a Bruknmank sonicator for 10, 15 and 30 mins respectively at room temperature. The dispersion studies were carried out at 10, 15, 30, 45, 60 minutes respectively in order to co-relate its effect before shear, during shear and after shear.

3.1.4. Fourier Transform Infrared Spectroscopy:

The MFC were examined for spectroscopic analysis using FTIR spectroscopy ATR mode (Shimadzu/IR prestige 21). The samples were analyzed keeping air as the reference. Scanning was done at the range of 4000 cm^{-1} to 500 cm^{-1} with a resolution of 4 cm^{-1}.

3.1.5. X- Ray Diffraction:

The X-ray diffraction pattern of MFC was analyzed using X-ray diffractometer (PW3040, XRD-PANalytical, Philips, Holland).Cu-Kα radiation with wavelength 0.154 nm was used as a source. The instrument was operated at 30 KV and 20mA.Scanning of the samples was done at 5° - 70° (2θ) with a rate of 5° (2θ) /min. The analysis was performed at the room temperature.

3.1.6. DSC/TGA:

The differential scanning calorimetric and thermo gravimetric analysis (DSC-TG) analysis were carried out using thermal analyzer (Netzsch, Germany) by heating the sample at 10 °C/min in argon atmosphere were the mass of the substance is recorded continuously as a function of temperature or time which gives us the thermal decomposition curve. DSC-TG provides information about the Decomposition, Kinetics, Purity check and Thermal stability of the sample.

3.1.7. In-vitro cytotoxicity:

Dried MFC samples of weight 10mg were used for this study. The samples were sterilized prior to use. Adipose derived stem cells (ADSCs) maintained in low glucose DMEM media supplemented with 10% FBS and 1% antibiotics were used for assaying the in-vitro cytotoxicity of the samples. Upon confluency these cells were trypsinized and 10^4 cells/well were seeded. The ADSCs were cultured in complete media (DMEM, low glucose, supplemented with FBS) under 5% CO_2 atmospheric conditions. Samples were assessed for their bio-compatibility for 48 hours. The presence of viable cells was determined through MTT assay by adding DMSO and taking the absorbance at 590 nm respectively [15].

4.1.RESULTS AND DISCUSSIONS

4.1.1. Shape and morphology:

This study demonstrate that the MFC fibers are disperesed as micron sized-aggregrates with few fibers disperesd and few entangled to each other.

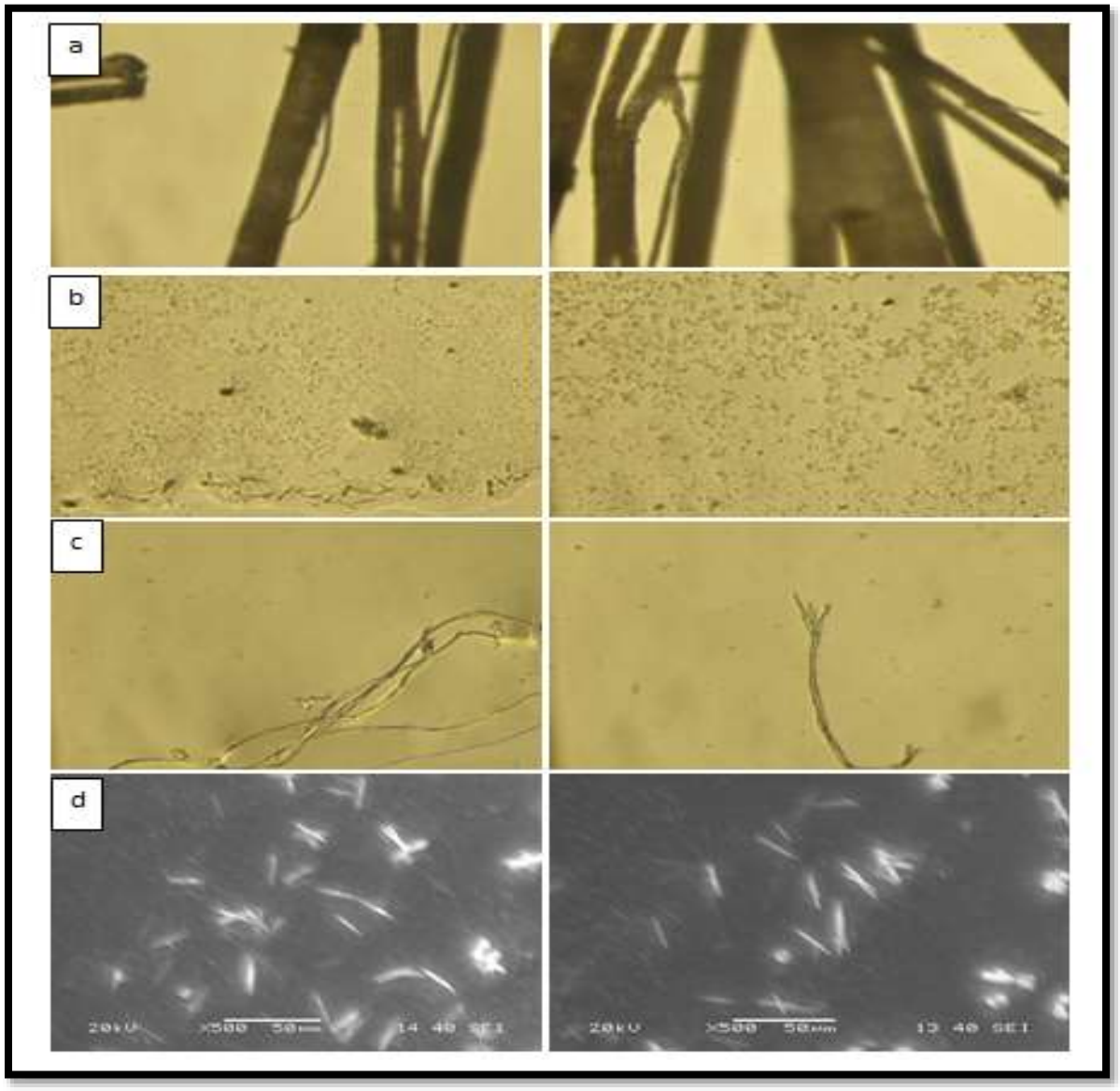

Figure 3: Optical images (at 20 X) while processing (a, b, c) and SEM images after processing (at 500X) (d).

4.1.2. Phytochemical test:

Jute by products is used extensively for cosmetics and medicines. Hence the extracted product could be utilized if it had some medicinal by-product in it.

Table 2: Phytochemical tests performed

S.NO	NAME OF THE TEST	EXPECTED COLOUR	RESULT
1.	Test for tannins	Dark Blue Colour	--
2.	Test for saponins	Foam appears	-
3.	Test for alkaloids	Yellow Colour precipitate	++
4.	Test for Flavonoids	Yellow Colour	+++
5.	Test for quinines	Red Colour	+++
6.	Test for steroids	Brown ring at interface	++
7.	Test for terpenoids	Reddish Brown at interface	-

Where, +++ highly present; ++ moderately present; - not present

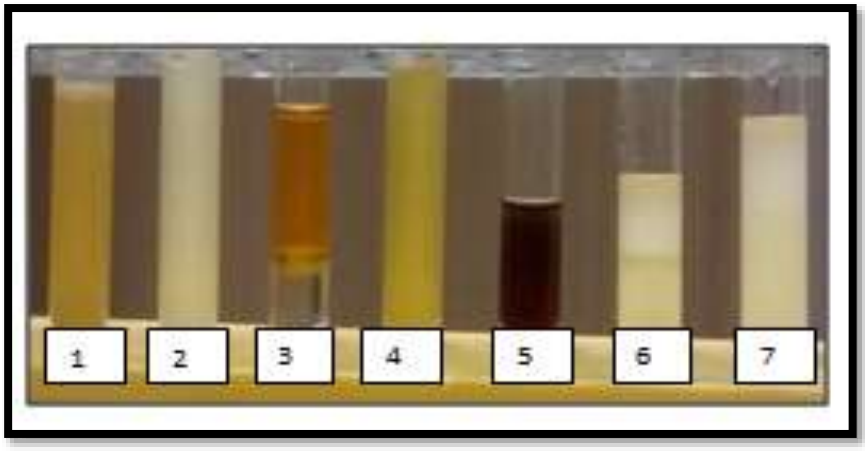

Figure 4: Phytochemical test results of the jute extract (after de-lipidization)

From the data above it was found that, after de-lipidization, the jute extract contained mostly flavonoids, quinines and also some amount of alkaloids and steroids. Flavonoids are phenolic compounds which act as primary antioxidants or free radical scavengers and can impart therapeutic activity such as antioxidant, anti-diabetic and anti-ulcer properties[36]. Presence

of steroids may either have a positive or negative effect depending upon the class of steroids present. The most common class of steroids present in plants is saponins which forms a foamy layer which is not found in jute, though the steroid test was positive[37]. This confirms that the absence of saponins subsidizes the negative effect and hence the jute extract can yet be used for medicinal purpose. Alkaloids and quinines also are used for anti-allergic, anti-cancer and anti-malarial purposes[38]. Thus, this study confirms that the by-product in process of cellulose extraction can be utilized for medicinal purposes after processing it.

4.1.3. Dispersion studies:

The structure MFC contains the hydroxyl groups in the equatorial position, on the cellulose chain protruding laterally. This position makes it readily available for hydrogen bonding. But the hydrogen bonds cause the chains to group together into a highly ordered structure forming a packed fibril (cylinder-like structure)[39]. The inter-chain h-bonds in between these are so strong that they surpass the H-bonding with water molecules. This bonding is also responsible for imparting the high mechanical strength to MFC, and preventing it from melting (i.e. MFCs are non-thermoplastic rather it is thixotropic)[40]. The MFC structural arrangement adds another feature; of swelling in water (i.e. they are very hygroscopic).

Figure 5: Dispersion study of MFC in various organic solvents a. 10 mins and b. 15mins after sonication, c. 30 mins and d. 45 mins of gravity settling

Table 3: Inference of solvents used for dispersion

S.NO.	SOLVENTS USED	INFERENCE
1	Methanol	*
2	Acetonitrile	*
3	DMSO	DMSO is also a good (non-derivative) dispersing agent for cellulose also it swells cellulose even two times more than water
4	DMF	DMF is a common solvent used in electrospinng it makes them swell and suspends MFC and CNT.
5	Chloroform	*
6	Toluene	*

Thus, the dispersion study was done in order to find a suitable solvent for dispersion. According to literature, DMSO and DMF serve as the best solvents for MFC dispersion without and modification in the MFC structure which was found similar in our study too[41]. MFC dispersed in methanol and acetonitrile during sonication but after 30 minutes of sonication, they eventually settled due to gravity. For toluene and chloroform, the MFC formed aggregates before, during and after sonication[42]. This is because in case of a non-polar solvent like toluene and chloroform, the ions do not dissociate but are preserved, because of the strong inter-bonding in the MFC structure[43]. This leads to MFC aggregate formation difficult to break. The dispersion of MFC in such solvents can be achieved by adding surfactants in order to transform the steric repulsion in toluene and chloroform and promote the compatibility with MFC.

4.1.4. FTIR Studies

The FTIR study helped in evaluating the presence of cellulose, hemicellulose and lignin present in our synthesized MFC on the basis of the functional groups present in the molecule.

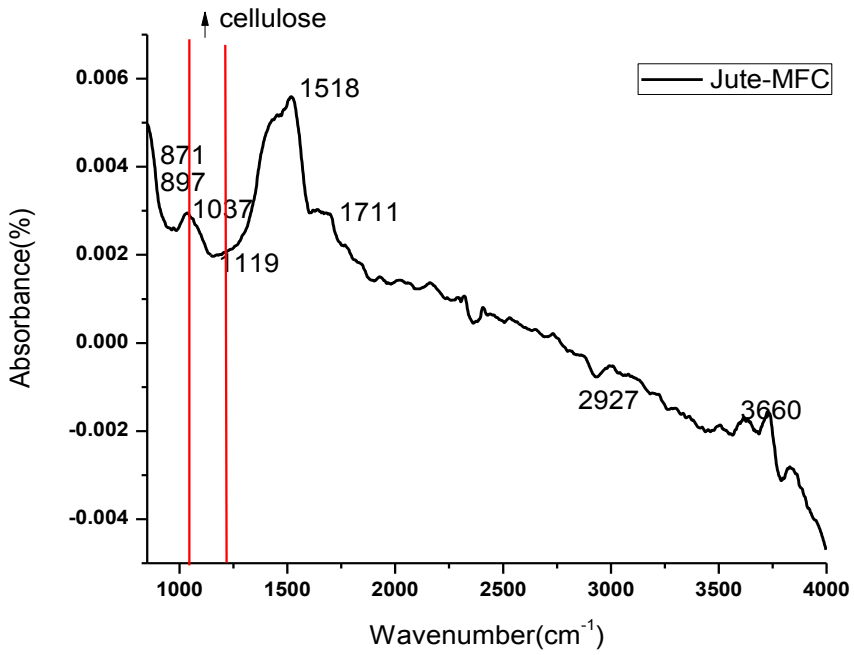

Graph 1: FTIR spectra of MFC

Table 4: FTIR of MFC with functional groups and their respective wavenumbers

S.NO.	FUNCTIONAL GROUPS	WAVENUMBER(cm^{-1})
1	antisymmetric out-of-phase stretching of glucose ring in cellulose	871 cm−1,
2	represents glyosidic C1 H deformation, with a ring vibration contribution and– O H bending	895 and 897, 1061 cm−1
3	higher cellulose content	1035 cm−1
4	which could be associated to the C O C stretch of the _-	1118 cm−1,

	1,4-glycosidic linkage in cellulose, was most prominent in MCC, Followed by pre-treated flax.	
5	suggesting the effective removal of hemicelluloses in the hydrolyzed	1256 cm−1 peak,
6	asymmetric CH2 bending and wagging	1352 cm−1
7	CH2 bending.	1428 cm−1
8	carbonyl groups	1601 and 1410 cm−1
9	absorption of water	1640 cm−1
10	COO^- asymmetric stretching	1735 and 1251 cm−1
11	C H stretching.	2900 cm−1
12	H-bonded of the OH groups	3000–3600 cm−1

From our synthesized MFC, spectra in the range of 1000 to 1035 cm^{-1} confirms the presence of cellulose[44]. Absence of peaks at 1256 cm^{-1} again confirms the removal of hemicellulose. Peaks in the range of 1119 cm^{-1} are a characteristic stretch due to presence of lignin, which is the reason for micro fibrillated shape of our cellulose[45]. Hence, this study confirms the formation of MFC from jute as a source.

Also from the above data we can see a shift in the bands from 870 to 1035 cm^{-1} which is due to the characteristic shift from cellulose I to cellulose II confirming presence of cellulose II which accounts to the micro fibrillated structure.

4.1.5. XRD studies

XRD is used to know the arrangement of atoms or molecules in the internal lattice of crystalline structure.

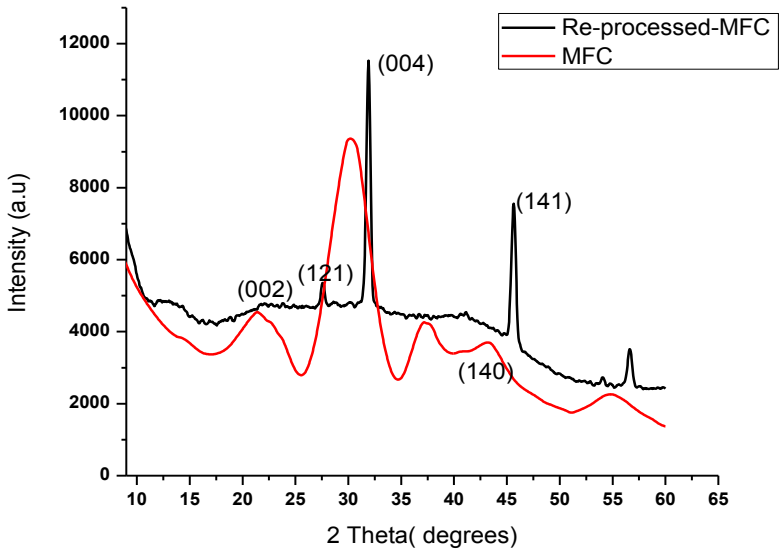

Graph 2: XRD of a. MFC batch 1(Red) and b. Reprocessed MFC (black)

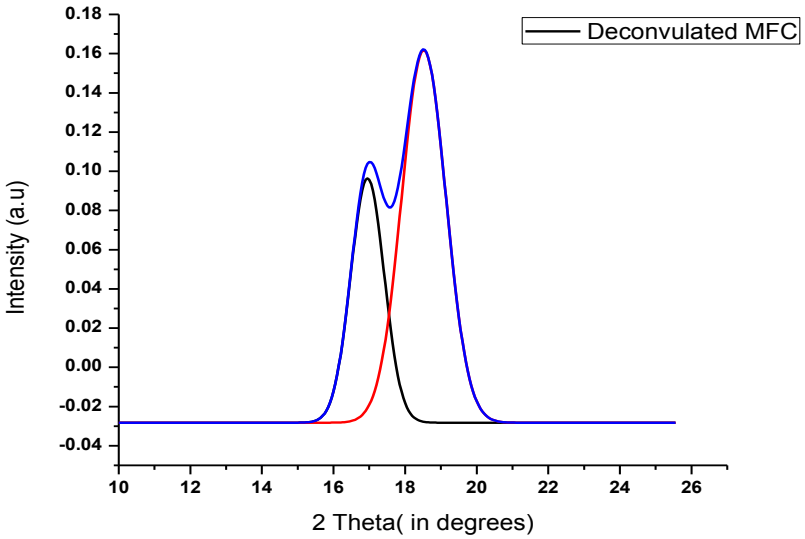

Graph 3: XRD of Deconvulated MFC batch 1(Red)

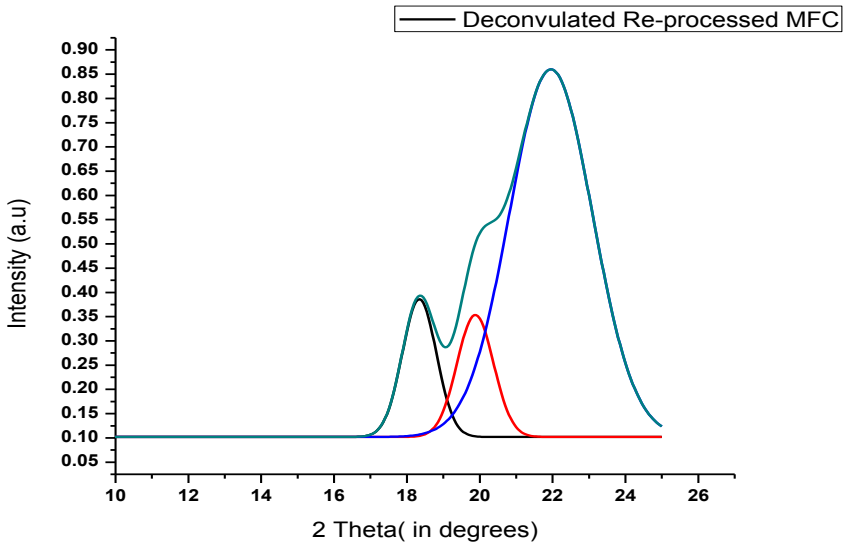

Graph 4: XRD of Deconvulated Reprocessed MFC (black)

Table 5: Crystalline size of MFC

Sample	2 Theta(in degrees)	Crystalline Size(in nm)
MFC-batch1	21.82	0.19
	30.13	0.89
Re-Treated MFC	22.19	0.50
	32.03	0.38

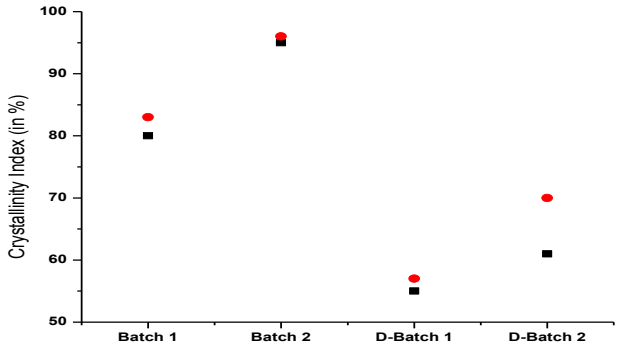

Graph 5: Crystallinity index of MFC batch 1(Red) along with Reprocessed MFC (black)

The XRD analysis shows that the synthesized MFC is mostly crystalline. According to literature, the MFC peaks are prominent at 16 º to 18º which confines to (121) plane of cellulose type II and the main cellulose peak is found in the range of 22.1º to 24.5º confines to (004) plane of cellulose type I. In our study we found peaks at 21.82 º and 30.13 º in the first synthesized batch of MFC[46].In the re-processed batch of MFC more crystalline peaks were found in the range of 22.19º and 32.03º respectively. A very low intensity peak was found at 18 º in both the batches. This confirms the presence of cellulose type I which is associated to micro fibrillated cellulose. Also from the crystallinity index plot it is found that the percentage falls around 75-80 for both the batches, confirming cellulose II in it.

The peaks were further deconvoluted in the range of 10 º to 26º to obtain the instrumental true spectrum (i.e. F_{tr}) from the measured spectrum (F_{ms}).

The following can be inferred from the Deconvoluted graphs:

1. In the Deconvoluted MFC, two sub peaks were obtained.
2. In the re-processed MFC, three sub peaks were obtained. This confirms that re-processing of the MFC, made our sample more crystalline with prominent peaks[47].
   The difference in area between the 1st and 2nd batch of MFC is 20%.

Also, the percentage crystallinity index of both the 1st batch MFC and re-processed MFC was plotted as shown above in Figure d.

4.1.6. DSC/TGA

Based on the thermal analysis of sample, i.e. the degradation of MFC with respect to temperature was analyzed.

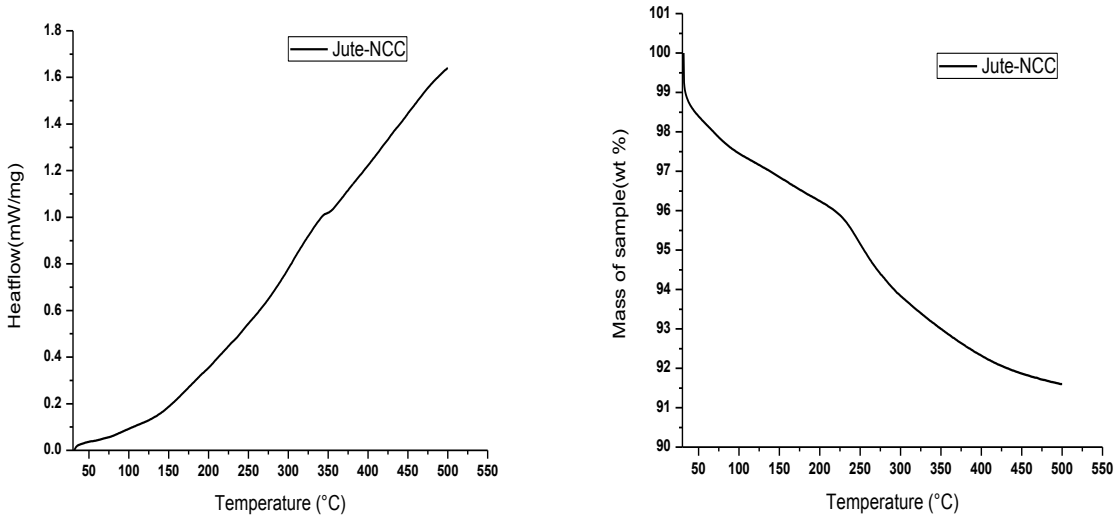

Graph 6: DSC/TGA spectra of MFC

According to literature, the Wax, pectin, and hemicellulose degrade at 180°C where as cellulose has a degradation in the range of 200- 390°C. In case of cellulose extracted from wheat straw and soy hulls the degradation was at 296 °C and 290 °C respectively[48]. Our, synthesized MFC showed degradation at 227 °C which confirms the presence of cellulose[49]. Also the data from the DSC, with degradation at 346.7 °C is in accordance with literature.

4.1.7. In-vitro cytotoxicity

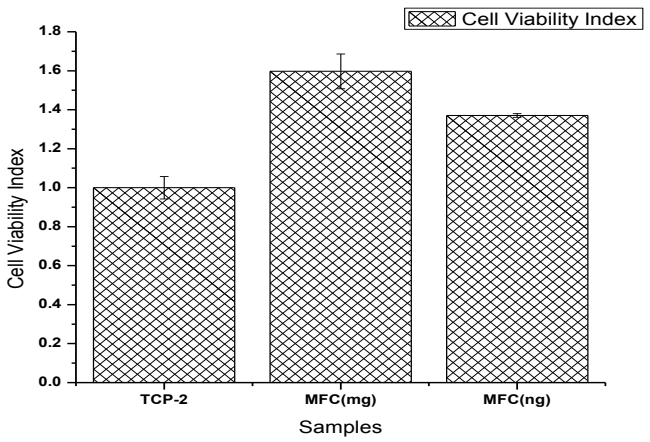

Graph 7: Cell viability index of MFC

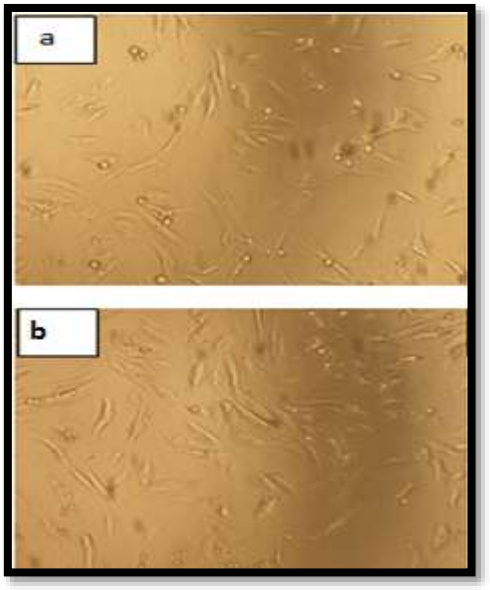

Figure 6: ADSCs cell proliferation in 24 hours a.TCP and b. MFC

The in-vitro cytotoxicity of micro fibrillated both in milligram and nanogram of the sample were observed using tissue culture plate as control .From the above data, it was observed that, MFC(in mg) showed more cell viability than MFC(in ng). Thus, it can be concluded that we can use good amount of MFC for load bearing applications in bone tissue engineering due to enhanced cell proliferation much more than control too.

Chapter 2

SPIDER SILK AND COCOON SILK (*Bombyx mori)*

1.5. Silks have been employed in tissue engineering for years as it possess extraordinary mechanical properties due to a combination of strength and extensibility that are superior to most man-made fibers[50]. These fibers are a protein-based material produced in a highly sophisticated hierarchical process under mild conditions[51].

1.6.Spider Silk:

Spider Silk is one of the most versatile and indispensable biomaterial ever known to mankind. The mechanical and mesoscopic properties of spider silk are incredible. Silk obtained from *Bombyx mori* also displays a broad spectrum of strength, although its mechanical hardness, tensile strength and Young's modulus are less than that of Spider Silk. Spider Silk has an intensely high amount of tensile strength and an equally high value of Young's Modulus[52]. It is one of the strongest material and having said that one can assert that its applications are not just confined to a small area but span over larger domains of engineering and technology.

1.7.Spider silk in bone tissue engineering:

Spider Silk can serve as scaffolds for tissue engineering and as drug delivery matrices. Besides, it has wide applications in bone engineering wherein it can be an outstanding material to be used for ligaments and tendons[53]. Beyond the biotechnological realm, it has a myriad of applications in aviation, infrastructure, civil construction and various other prospective areas. Hitherto we have just discovered this immense potential concealed in the Spider Silk and have not yet unleashed its entire potential. Researchers across the globe are trying hard to discover certain more specific applications so that we can transcend beyond our infancy phase and can yield better out of it.

1.8.Structure of Spider silk:

This structural strength of Spider Silk is well manifested in the molecular arrangement of atoms and the secondary structures that form the Spider Silk protein called Spidroin. The Spidroin protein has a characteristic sequence motif comprising of repeats of alanine (An) and alternating Gly-Ala as well[54]. These primarily form beta sheets. These beta sheets are stacked upon one another to form a pile. There are other pre-stressed chains and random coils that are interspersed in a matrix. The beta stacks are linked by these short regions in a serial arrangement thereby imparting the silk its incredible strength[55].

Recently, researchers have produced a variant of silk that is even stronger than the naturally obtained one. This was achieved by spraying the spiders with an aqueous solution of Carbon Nanotubes (CNTs) and Graphene flakes[56]. The silk that was produced by such spiders had a comparatively higher tensile strength than the normal ones. It was conjectured that the CNT and graphene was absorbed by the spider's body and somehow made its way into the silk. However, the exact mechanism and process of how the added nanomaterials penetrated the body and then finally entered the silk still remains a mystery. A lot of research has been done in order to determine the properties of Spider Silk and much of them focused on understanding of what renders the silk its strength

There has been considerable work on dissolving the spidroin in various solvents and then regenerating the silk fibers in order to assay its mechanical, thermal and structural features. For this purpose both benign and strong solvents have been used and it has been inferred that the choice of solvent greatly influences the secondary structures of the spidroin protein. Certain solvents like methanol lead to an increase in the formation of beta sheets and others like HFIP have the reverse impact, that is, they show a lesser percentage of beta sheets and rather display higher alpha helix content. Actually, the solvent that is used to dissolve the spidroin protein causes distortion of the secondary structures. Secondary bonds are cleaved and the protein loses its native structure. Hence it is of paramount importance that we wisely choose the solvent such that it does not lead to a degradation of the structure and retains the conformation and crystallinity of the protein. One such solvent is a mixture of $CaCl_2$, Ethanol and Water in the molar ration 1:2:8. This particular solvent is the best insofar as retention and preservation of structure and conformation of the protein is concerned.

Spider Silk and amyloid fibers have been combined to form a composite that has better structural features. Films of spider silk and amyloid were prepared and it was found that the orthogonal arrangement of beta strands in the two proteins was chiefly the reason behind the strength[57].

Researchers have been struggling to obtain the silk from a reliable source. Some have genetically engineered the spidroin and developed a recombinant protein and compared it with the natural one. Albeit it displayed relatively appreciable properties yet it failed to give a perfect match. So, the toughest challenge being faced it production of silk, either synthetically or naturally, such that it can at least resemble the natural spider silk, if not better. In one research, the silk was directly

obtained from the spider. *Nephilus* was used for this purpose. It was sedated with CO_2 and then pinned to a scaffold. The silk was then gently pulled out with a tweezers from the spinneret and then attached to a motor that rotated at a slow rpm. This way, about 30-80 meters of the silk was obtained. Until now, none has used the silk to assay its cytotoxicity and biocompatibility.

1.9.Mechanical properties of Spider silk:

The silk of spiders cannot be collected as easily, but the nets of orb weaving spiders (***Araneidae***) have been employed for various applications due to their outstanding mechanical and biomedical properties. Orb webs can be found all over the world, with web diameters ranging from a few centimeters to several meters. Spider silks are tailored for specific purposes and exhibit a great variation in mechanical properties. Between the different silk types their strength (the stress needed to break the fiber) ranges from 0.02 to a remarkable 1.7 GPa, which exceeds steel (1.5 GPa), while the extensibility varies between 10 and 500 %. Interestingly, most spider silks have a sophisticated combination of strength and extensibility, which yields a very high toughness (the amount of energy absorbed per volume before breakage) that exceeds most natural or man-made fibers[58].

The orb-weaving spiders produce a variety of high-performance fibers with mechanical properties that outperform synthetic materials in the combination of strength and elasticity[59]. Dragline silks form extremely strong fibers. Dragline silk tensile strength is comparable to Kevlar and it has extensibility which is seven times greater than the extensibility of Kevlar.. This combination of features makes major ampullate silk one of the toughest materials known. Minor ampullate silk is similar to major ampullate silk in tensile strength but has limited elastic behavior[60]. However, flagelliform silk has outstanding extensibility, stretching as much as 200% and, at the same time, it is a strong fiber summarizes the strength, elasticity and energy to break values for known spider silks along with selected biomaterials and man-made materials.

2 .1 MATERIALS AND METHODS

2.1.1. Materials:

Spider silk was collected from homemade spider webs. Sodium Hydroxide (NaOH), Ethanol (99%), Lithium Bromide (LiBr) was purchased from S.D.Fine – Chemicals Ltd.Cocoon of *Bombyx mori* grade was purchased from. Same ADSCs were used as in Chapter 1.

2.1.2. Methods:

2.1.2.a. Extraction of Spidroin from Spider silk:

For extraction of spidroin from spider silk we used 3 different benign solvents namely, 20 % ethanol, 10 % NaOH and 9.3 M LiBr. The collected spider web was first separated from dust and un-wanted particles stuck on it. After this the web was broken into small pieces, weighed and then the above solvents were added to it in a 50 ml falcon tube. The falcon tube containing the spider web was then vortexed and then centrifuged at 3000 rpm for 10 mins. This process was repeated 3-4 times for extraction of the solvents via application of centrifugal force. The solution was then stirred overnight in a beaker for extraction of more protein in the same solvent. After this, the solvent containing the web was then filtered using a Whattman Filter of 2.5 micrometer size to remove the undissolved web. After this, the filtered extract was then re-filtered using a 0.45micromtere PTFE filter. This process helped in removing the small particles leaving out the protein extract. This extract was then dialyzed, for 12 hrs repeatedly changing distilled in every 2 hours till neutral pH. After dialysis, the extracted protein was stored in falcon tubes at 4°C for further study.

3.1. CHARACTERIZATIONS OF MICRO FIBRILLATED CELLULOSE:

3.1.1. Bradford assay for Protein Estimation

The Bradford assay, is a colorimetric protein assay, whose principle is based in the shift in absorbance of the dye Coomassie. The red form of coomassie reagent changes to blue and gets stabilized by binding with the proteins. At 595 nm the bound form of the dye exhibits absorption maxima. The unbound (cationic) form is generally green /red and upon binding with protein it stabilizes to form a blue anionic state. Absorbance at 595 nm is proportional to amount of bound dye and thus, also to the amount of protein present in the sample, with which we can determine the concentration[61].

3.1.2. FLUORESCENCE SPECTROSCOPY

Fluorescence spectroscopy or spectro-flurometer is a type of spectroscopy which analyses fluorescence of the samples using a beam of ultraviolet light that measures the emission energy after the molecule has been irradiated into an excited state which is detected by the fluorimeter. It is basically used to study solvent-protein interaction. To detect the presence of proteins in spidroin and fibroin we used a protein binding dye called ANS[62].

ANS (8-Anilinonaphthalene-1-sulfonic acid) dye is an amphilic dye containing both sulphonic and amine groups in its structure. ANS is non-fluorescent in water, but is exhibits fluorescent upon binding with proteins or membranes. This property of ANS makes its usage as an indicator for protein detection, its folding, and conformational changes. The large increase in fluorescence and quantum yield and the pronounced blue shift of the emission maxima has made ANS an extensively used probe to detect the surface hydrophobic binding sites of a protein[63].

The dry spider web was taken in a glass slide and to it 200microlitre of ANS dye was added and left to incubate for 5-7 minutes after which it was washed with distilled water and observed under the microscope. Images of cob web prior to staining were taken using simple laboratory microscope.

3.1.3. FTIR

The spidroin and fibroin proteins isolated were examined for spectroscopic analysis using FTIR spectroscopy ATR mode (Shimadzu/IR prestige 21). The samples were analyzed keeping air as the reference. Scanning was done at the range of 4000 cm^{-1} to 500 cm^{-1} with a resolution of 4 cm^{-1}.

3.1.4. CD

Circular dichroism (CD) is a spectroscopic study used for estimation of the protein secondary structure. Both qualitative as well as quantitative data can be recorded using this. The principle of CD is based on absorption of optically active chromophores in relation to the difference in the amount of right and left polarized light. This difference in absorbance may either be a positive or negative absorption spectrum[64].

Circular Dichroism (CD) spectra of the isolated proteins were recorded using a JASCO J-810 CD polarimeter (JASCO, Tokyo, Japan. The spectrum represents an average of two accumulations recorded in a range of 190-250 nm, with resolution of 0.2 nm, bandwidth of 0.5 nm, response time of 4 s, sensitivity of 100 mdeg, and a scan speed of 20nm/min using a cuvette of path length 1mm. All the measurements were recorded at 25°C. The percentages of the different secondary structure components (α-helix, β-sheet and random coil) via Yang's and Reeds were estimated (prediction errors on the range of 190-200 nm were 5%) in online k2D software.

3.1.5. *In-vitro* Cytotoxicity

Extracted protein, spidroin and fibroin samples of concentration 10mg/ml were used for this study. The samples were sterilized prior to use. In this study also ADSCs were used similar to Chapter 1.

4.2.RESULTS AND DISCUSSIONS

4.2.1. Bradford assay for Protein Estimation

The concentration of the proteins, were found using Bradford assay using BSA (Bovine serum albumin) protein for plotting the standard curve. By plotting the calibration curve we found the concentration of proteins isolated by various benign solvents as tabulated below.

Table 6: Protein concentration via Bradford assay.

Sl No.	Type of silk	Solvent dissolved in	Weight of silk(g)	Total vol (ml)	Conc (µg/ml)
1	Spider Silk	Distilled water	1.5	25	-
2		10% NaOH	0.7	7.5	60
3		9.3 M LiBr	0.5	26	19
4		20%Ethanol	0.35	25	33
5	Cocoon	9.3MLiBr	5	50	15

4.2.2. FLUORESCENCE SPECTROSCOPY

The dried spider webs image was taken both before and after staining with dye.

Figure 7: Optical microscopy of spider web at 20X

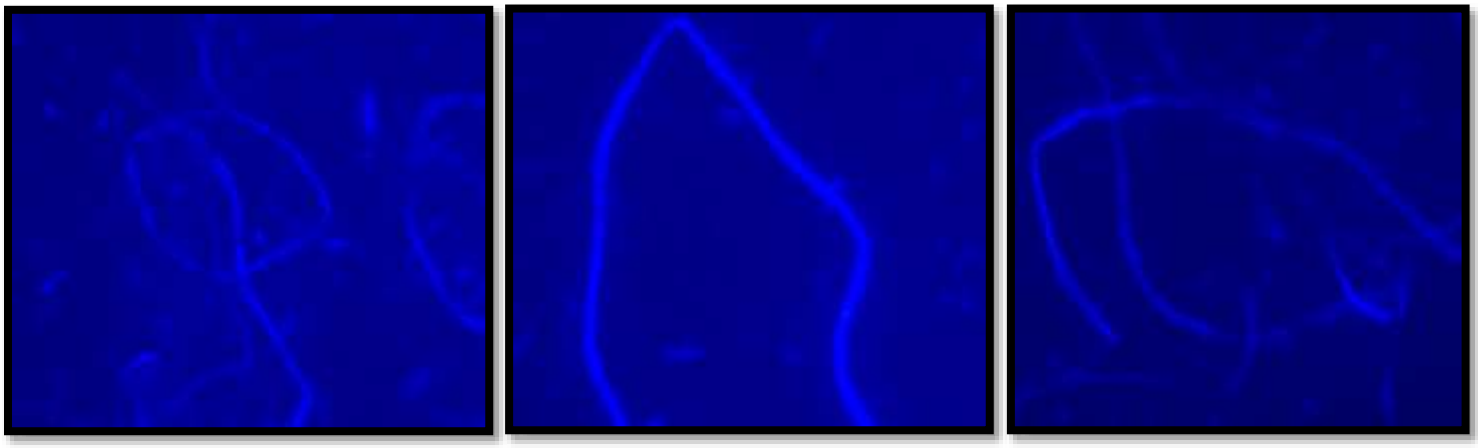

Figure 8: Fluorescence microscopy of ANS-dyed spider web

From the images it is prominent that the cob web has proteins in it which is determined by further study using FTIR and CD to confirm the presence of spidroin and fibroin.

4.2.3. FTIR

The FTIR spectrum of all the samples with transmittance versus wavenumber from 4000 to 600 cm $^{-1}$ along with the deconvoluted spectra with absorbance versus wavenumber from 1600-1700 cm $^{-1}$ has been plotted.

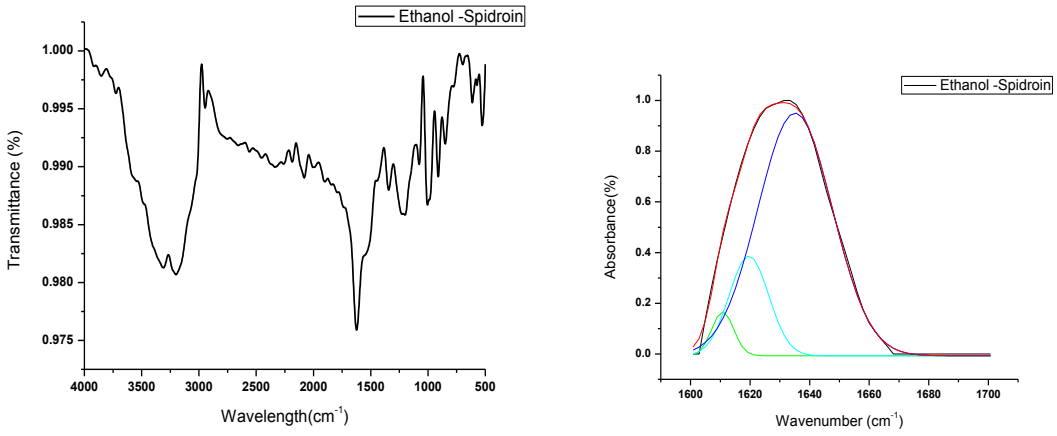

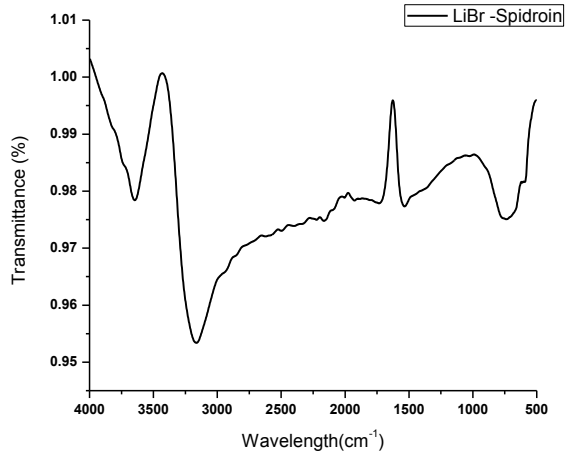
LiBr -Spidroin
Transmittance (%)
Wavelength(cm-1)

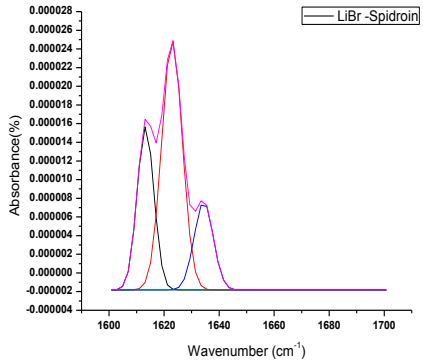
LiBr -Spidroin
Absorbance(%)
Wavenumber (cm-1)

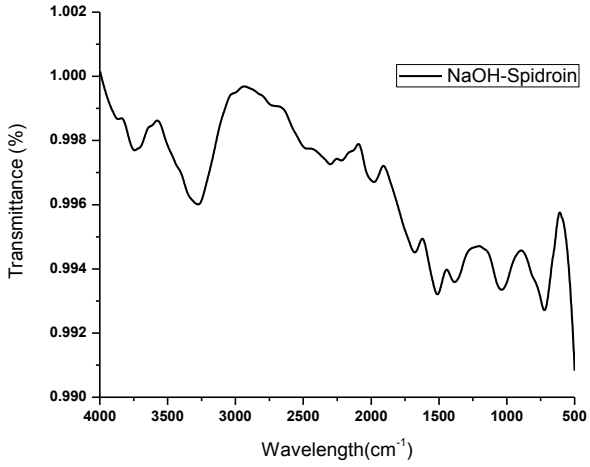
NaOH-Spidroin
Transmittance (%)
Wavelength(cm-1)

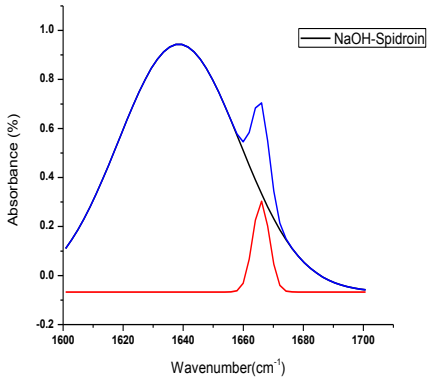
NaOH-Spidroin
Absorbance (%)
Wavenumber(cm-1)

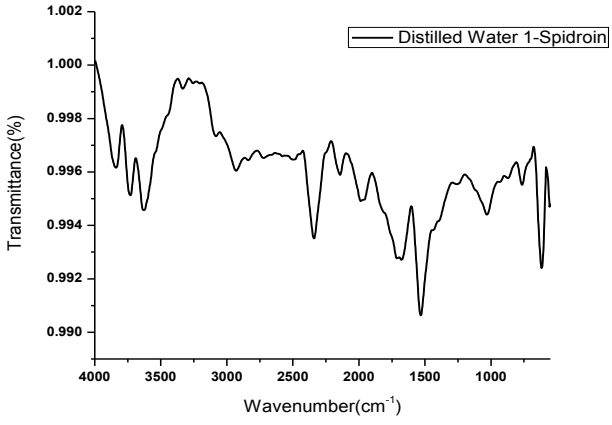
Distilled Water 1-Spidroin
Transmittance(%)
Wavenumber(cm-1)

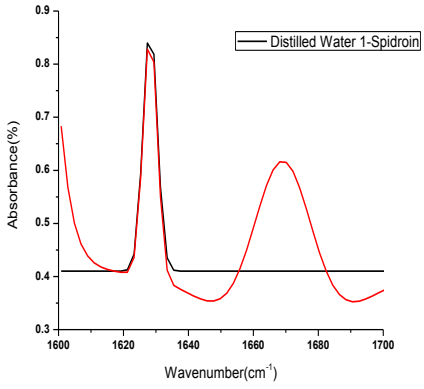
Distilled Water 1-Spidroin
Absorbance(%)
Wavenumber(cm-1)

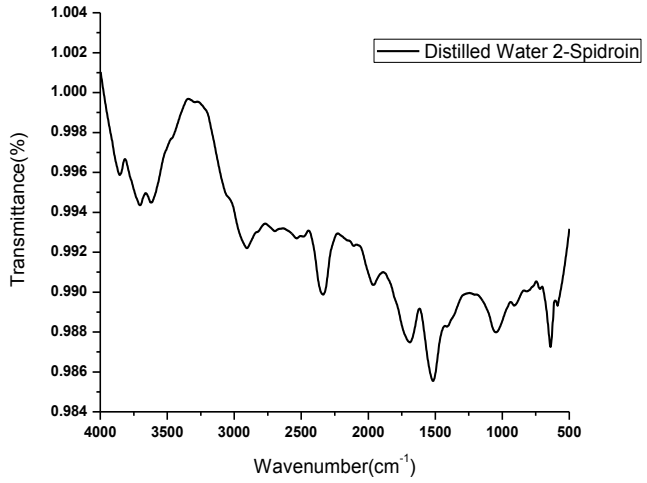

Graph 8: FTIR spectra of proteins along with deconvolution

From the above graphs, on the basis of stretching of functional groups, the amount of secondary structures present in spidroin and fibroin has been evaluated.

Table 7: Percentage of Secondary structures via Deconvolution of FTIR

Secondary Structures		**Spidroin In Ethanol (in %)**	**Spidroin In LiBr (in %)**	**Spidroin In NaOH (in %)**	**Spidroin In DW 1 (in %)**	**Spidroin In DW 2 (in %)**	**Fibroin In LiBr (in %)**
b-Sheets	(1616-1637 and1697-1703)	15.59	36.07	9.12	NA	94.87	36.50
a-Helix	(1653-1662)	0.0	0.0	0.0	NA	0.0	0.0
Random Coils	(1637-1652)	78.73	0.0	0.0	NA	0.0	57.19

b-Turns	(1663-1696)	0.0	0.0	94.36	NA	0.0.	0.0
Others	(1595-1615)	17.82	17.82	0.0	NA	0.0	0.0

4.2.4. CD

The CD spectra of all the protein samples were recorded in the range of 190 to 250 nm. According to literature, the CD spectra of any spider silk protein, spidroin is found in the range of 194-197 nm due to negative cotton effect and around 210-219 due positive cotton effect depending on the optical rotation versus wavelength[65].

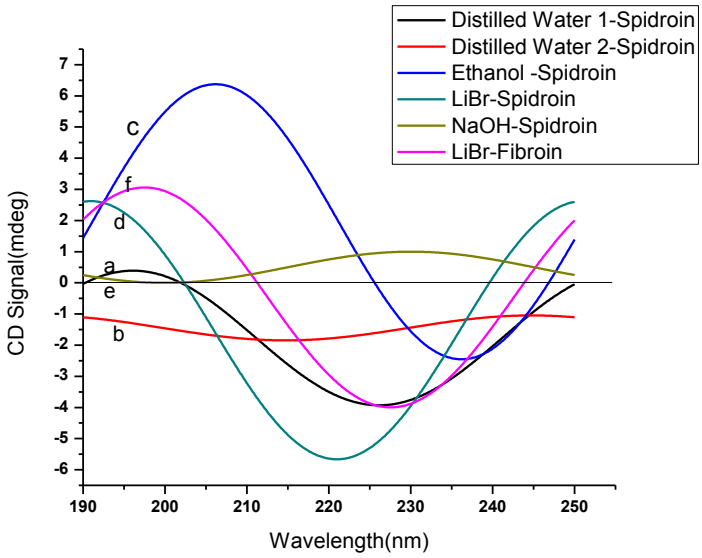

Graph 9: CD spectra of proteins

From the graph above the following was observed:

1. Distilled Water (Sample 1), there is a +ve increase in CD spectra around 197nm, which on increase in wavelength decreases with a –ve CD spectra at 217 nm. Both these peaks are characteristics of β-sheets.

2. For Distilled Water (Sample 2),–ve peaks around 197nm and 217 nm, are seen without much change in CD spectra with increase in wavelength. The presence **of** spidroin in such case is not certain, which in co-relation with FTIR data is also observed.
3. For Ethanol, a very high +ve peak at around 197nm and a –ve 217 nm peak, shows presence of β-sheets. The high intensity peak is indicative of more β-sheets, which is in accordance to FTIR data.
4. For LiBr-Spider Silk, a similar trend of +ve low 197 nm and –ve steep 217 nm peak was observed, indicative of β-sheets.
5. For NaOH, both +ve 197 nm and 217nm peaks are indicative of certain transitions between the β-sheets because of reaction with 10%NaOH along with free C-H groups of Spidroin.
6. For LiBr-*Bombyx mori*, the CD spectra trend is similar to Ethanol and LiBr-spidroin, indicating presence of good β-sheet content.

Table 8: Percentage of Secondary Structure via CD

Secondary Structure	Distilled Water 1-Spidroin		Distilled Water 2-Spidroin		Ethanol-Spidroin		LiBr-Spidroin		NaOH-Spidroin		LiBr-Fibroin cocoon	
	Yang's	Reeds	Yang's	Reeds	Yang's	Reeds	Yang's	Reeds	Yang's	Reeds	Yang's	Reeds
α-helix	31.2	0	19.5	0	27.6	0	24.7	0	0	0	45.5	0
B-sheets	0	57.5	14.2	49.1	0	0	32.3	61.8	0	0	0	100
Turns	35.1	0	32.4	0	72.4	100	24.7	0	0	46.9	52.6	0
Random coils	33.7	42.5	34.0	50.9	0	0	18.4	38.2	0	53.1	1.8	0

Thus, from the above data, and also from other studies it can be concluded that both spider silk and cocoon has spidroin and fibroin proteins respectively.

4.2.5. In-vitro Cytoxicity:

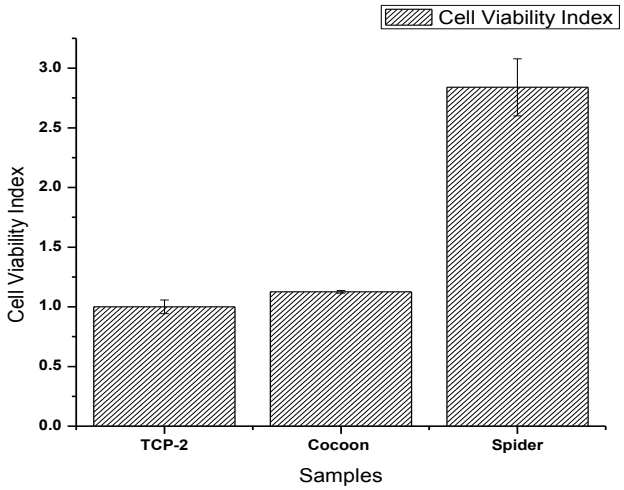

Graph 10: Cell viability index of proteins

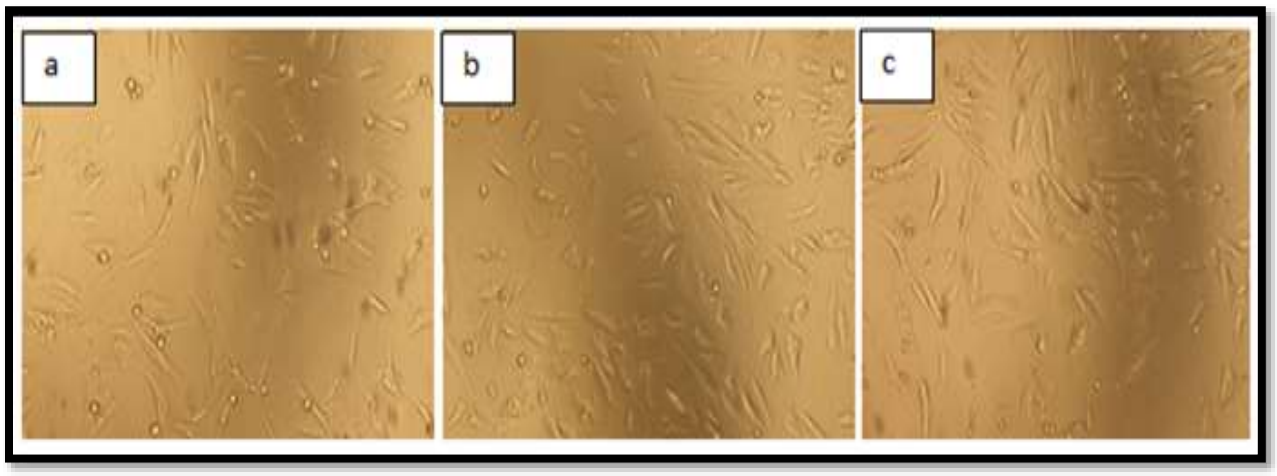

Figure 9: ADSCs cell proliferation in 24 hours a.TCP b. Spider and c. Cocoon

The in-vitro cytotoxicity of both the spider silk and cocoon silk were observed using tissue culture plate as control .From the above data, it was observed that, spider silk was more compatible than cocoon, whereas cocoon showed similar compatibility to that of control. Thus, we can conclude that spider silk induces cell proliferation.

Chapter 3

MAGNESIUM OXIDE AND ZINC OXIDE NANORODS

1.1. Bone defects due to osteoporosis are common in the aging -postmenopausal women which on severe cases often induces fracture. The major reasons for these are low cell attachment and proliferation and decrease in the collagen and osteocalcin levels[66]. This not only influences the present bone of the human body but also on implanting new bone this weakened bone imparts structural imbalance and stress on the bones . Research has been going on in this area to design novel orthopedic implants with multiple characteristics both in imparting bone formation and inhibiting bone resorption. Such inquisitive quality can be achieved by using high aspect ratio materials i.e. nanoscale materials which would provide shear shielding and promote osteoinduction[67].

Studies on designing such synthetic nanomaterials have gained recent success both in vitro and in vivo experiments. Such nanomaterials of titanium have shown to enhance cellular migration, and induce differentiation of bone cells. Apart from these the hollow tubes can also be used as a platform for drug carriers and immobilization of functional groups or growth factors to enhance its applicability in bone tissue engineering[68].

Magnesium oxide (MgO) is has simple structure and ionic bonding which makes it good for solid state and surface studies. It can be easily synthesized in the order of nanostructure. It has been found to show catalytic activity in many reactions due to small number of defect sites (steps, kinks, corners, etc.) with surface ions, particularly oxygen, having low coordination numbers. MgO in nanoparticle form has unique property. It has high surface areas and intrinsically high surface reactivity which allows these materials to be especially effective as adsorbents .Thus it can be good for bone tissue engineering[69].

ZnO has unique property of being optoelectronic materials in the ultraviolet (UV) region since it has wide bind gap (3.37 eV) and large excitation binding energy (60 meV). Nanoparticle, nanorods and nanowires, nanobelts are some of the ZnO nanostructures .ZnO nanotubes have lots many unique properties such as porous structure and large surface area. This unique property makes it good for applications as sensors. Furthermore it topographic feature makes it advantageous for use as drug carrier. Thus, it can be used in bone for implantation.

In our study, we have synthesized magnesium and zinc oxide nanorods and studied its effect on adipose derived stem cells.

1.2.Magnesium oxide nanorods:

MgO nanorods extensively used for load bearing application as they are not harsh to the human body as well have a high aspect ratio. MgO can be used as an effective reinforcement material along with hydroxyapatite or along with a polymer[70].

1.3.Zinc oxide nanorods:

ZnO nanorods has also gained commercial success in the area of miniaturized of pH sensors as nanoelectrodes due to its large surface-to-volume ratio which helps in short diffusion distance between the analyte and electrode surface. Also zinc oxide is non-toxic to human cells[71].

2 .1 MATERIALS AND METHODS

2.1.1. Materials:

Magnesium acetate, urea, Zinc nitrate hexahydrate and ammonia was purchased from S.D.Fine – Chemicals Ltd.

2.1.2. Methods:

2.1.2.a. Synthesis of Magnesium oxide nanorods

Hydrothermal synthesis method was followed to synthesize magnesium oxide nanorods. For this 6.44 g of magnesiumacetate was dissolved in 75 ml of distilled water and stirred on a magnetic stirred for 30 mins at room temperature. After the this 1.2 g of urea was added to it drop wise while stirring the mixture continuously at room temperature[72].30 ml of the above solution was then poured in a 50 ml Teflon holder and 20ml of space was left to avoid breakage due to pressure. This Teflon holder was then inserted in a steel autoclave, screwed tightly and kept inside an oven at 180 for 15 minutes for the reaction to happen. After 15 minutes, the Teflon autoclave was allowed to cool inside the oven eventually avoiding taken it out or switching of the power supply, rather the temperature was reduced slowly. After the system has cooled and reached at room temperature, the samples were transferred to falcon tubes and centrifuged at 8000 rpm for 10 minutes with repeated washing with distilled water and later with ethanol. The sample was then dried in a vacuum oven for 48 hrs.

After that this dried white powdered sample was then calcined at 600°C for 1 hr. to obtain the nanorods.

2.1.2.b. Synthesis of Zinc oxide nanorods

Similar to above again, hydrothermal synthesis method was followed to synthesize zinc oxide nanorods. For this 15 g of zinc nitrate hexahydrate was dissolved in 50 ml of distilled water. To this 20 g of sodium hydroxide pellets were added slowly and kept to stir in a magnetic stirrer for 8-10 hrs until a white coloured solution was prepared[73]. After this, 30 ml of this mixture was loaded in a Teflon autoclave and kept inside the oven at 90°C for 14 hrs. Upon cooling, the sample

was centrifuged at 8000 rpm for 10 mins washing it with distilled water followed by ethanol and kept for drying in vacuum oven for 48 hrs.

The dried powder sample was used for further studies.

Figure 10: Teflon autoclave for synthesis via hydrothermal method

3.1. CHARACTERISATIONS AND RESULTS:

3.1.1. SEM

3.1.1. a. MgO

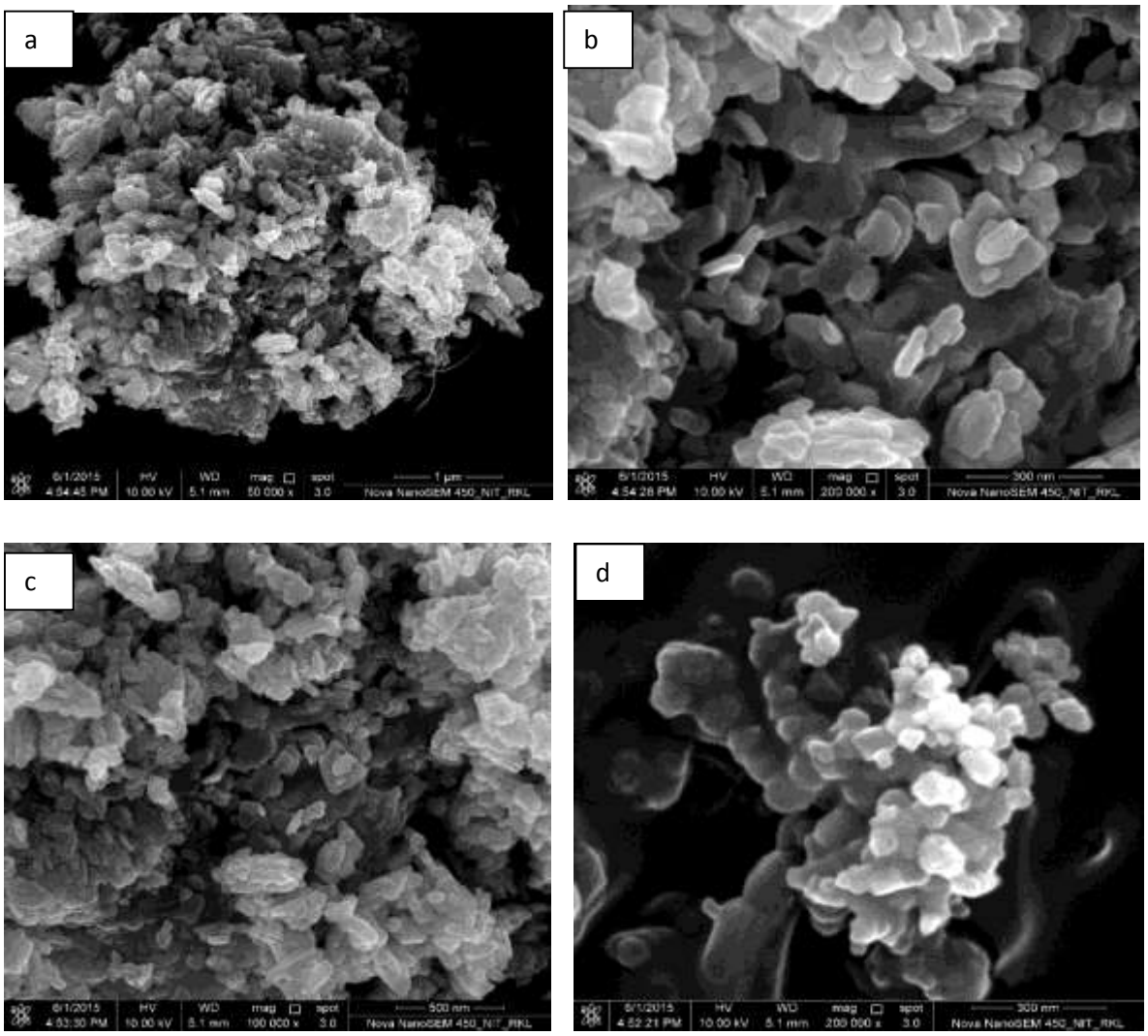

Figure 11: SEM image a. agglomerated MgO nanoparticle, b. agglomerated MgO nanoparticles forming MgO nanorods, c. and d. agglomerated MgO nanoparticles

From the above SEM images it is clearly visible that the formed MgO nanoparticles agglomerated to form MgO nanorods**.** a. shows the agglomerated nano particles, b. shows the nanorods with 300nm dimensions , c shows large amount of MgO agglomerates with 500 nm dimensions and d. shows an inside image of agglomerated nanoparticles.

3.1.1. b. ZnO

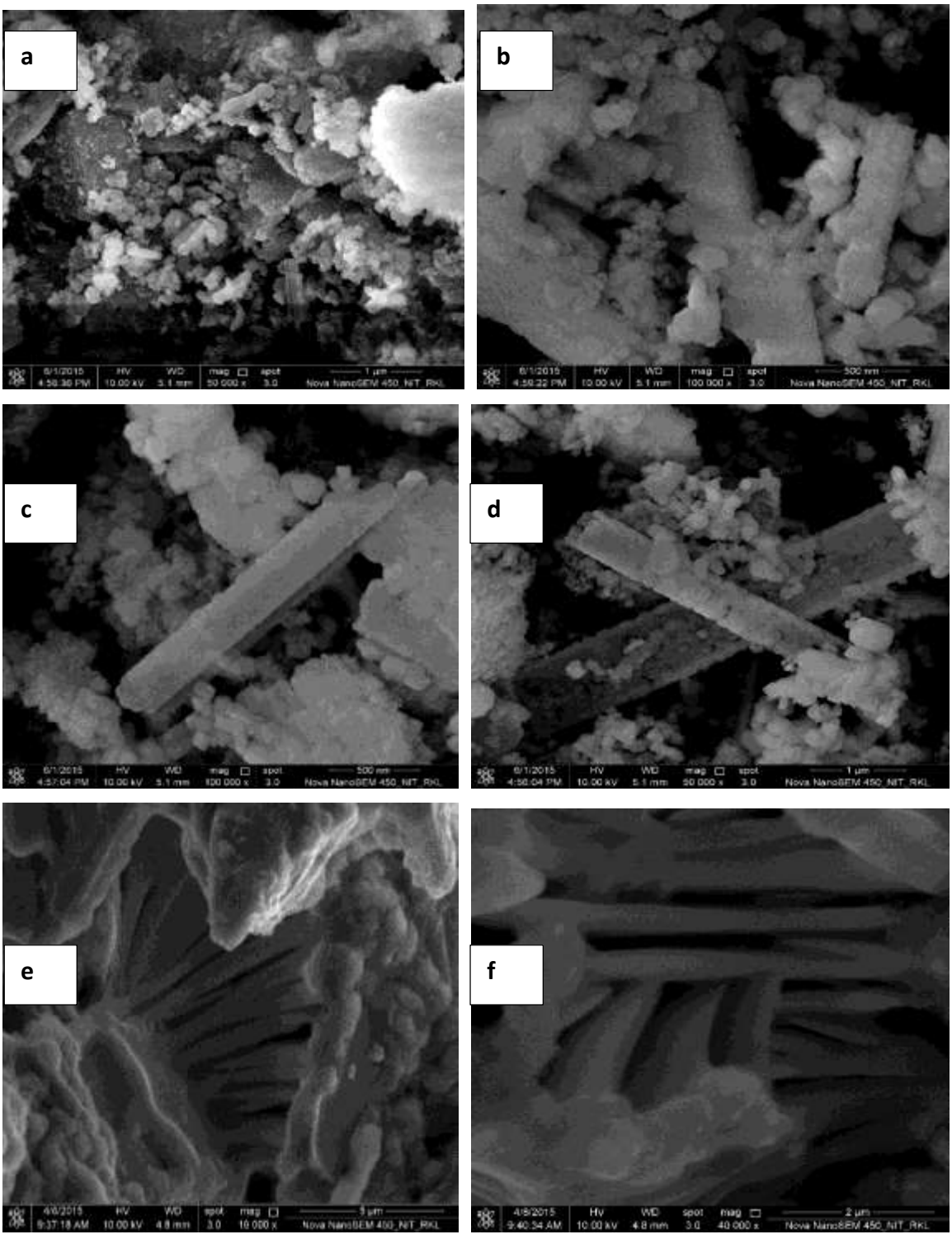

Figure 12: SEM image a. agglomerated ZnO nanoparticle, b., c. and d. agglomerated ZnO nanoparticles forming ZnO nanorods e., f. growth of ZnO nanorods

From the above SEM images it is clearly visible that the formed ZnO nanoparticles agglomerated to form ZnO nanorods in a similar manner to MgO**.** a. shows the agglomerated nano particles, b. shows the nanorods with 500nm dimensions , c and d also shows agglomerated nano particles which forms the nanorods, e and f confirms nanorod like structure formation.

3.1.2. XRD

The X-ray diffraction pattern of magnesium oxide nanorods and zinc oxide nanorods was analyzed using X-ray diffractometer (PW3040, XRD-PANalytical, Philips, Holland).Cu-Kα radiation with wavelength 0.154 nm was used as a source. The instrument was operated at 30 KV and 20mA.Scanning of the samples was done at 5° - 80° (2θ) with a rate of 5° (2θ) /min. The analysis was performed at the room temperature.

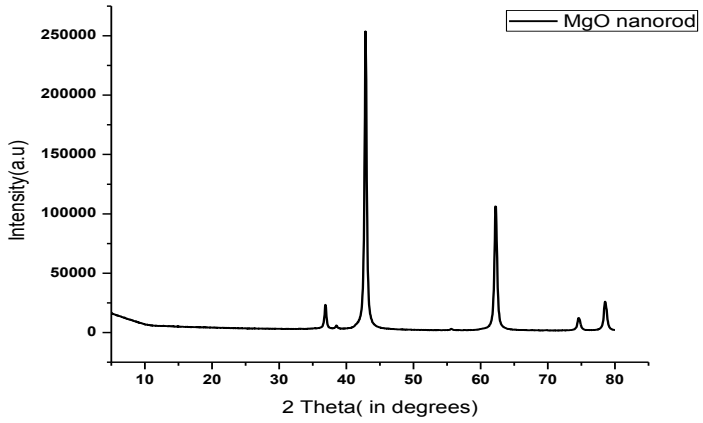

Graph 11: XRD of MgO

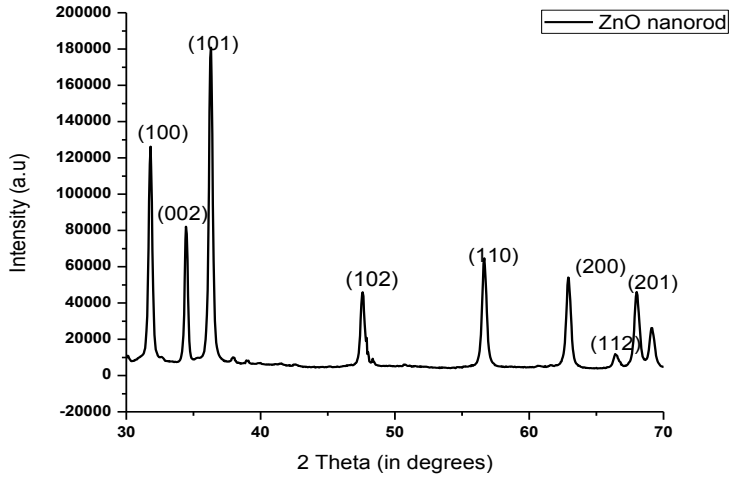

Graph 12: XRD of ZnO

Table 9: Crystalline size of MgO

Sample	2 Theta(in degrees)	Crystalline Size(in nm)
MgO	**37.23**	**0.5**
	42.82	**0.47**
	62.32	**0.44**
	74.69	**0.41**
	78.76	**0.43**

Table 10: Crystalline size of ZnO

Sample	2 Theta(in degrees)	Crystalline Size(in nm)
ZnO	**31.7**	**0.5**
	34.35	**0.59**
	36.28	**0.5**
	47.66	**0.51**
	56.71	**0.5**

The XRD analysis shows that the synthesized magnesium oxide nanorod is mostly crystalline. According to literature, the MgO nanorod peaks are prominent at 37 º, 42 º, 62 º, 72 º and 78º respectively which is exactly same in our data[69]. Similar was in case of zinc oxide nanorods which exhibited peaks at 31º, 34º, 36º, 47º and 56 º respectively. Also, the crystalline size was found using Scherer's formula which was found in the range of 0.45 nm for MgO nanorod and 0.5 nm for ZnO. Thus, it is evident that the material synthesized was MgO nanorod.

3.1.3. In-vitro cytotoxicity:

It was found that magnesium oxide nanorods were more compatible than zinc oxide nanorods after incubate for 24hr in adipose derived stem cells.

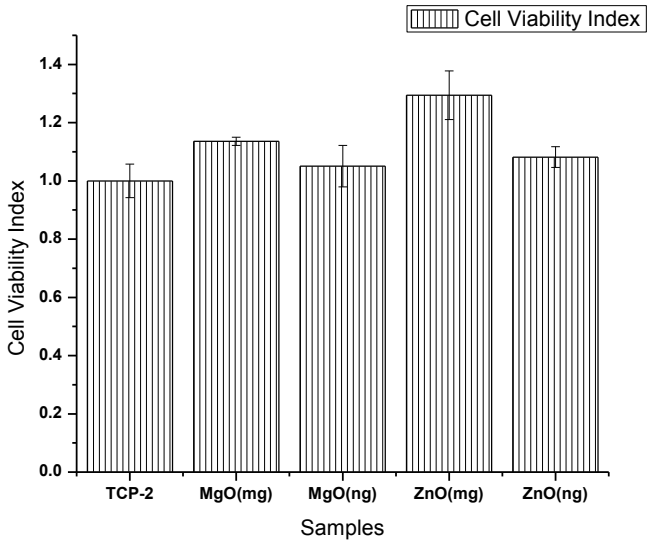

Graph 13: Cell viability index of MgO and ZnO

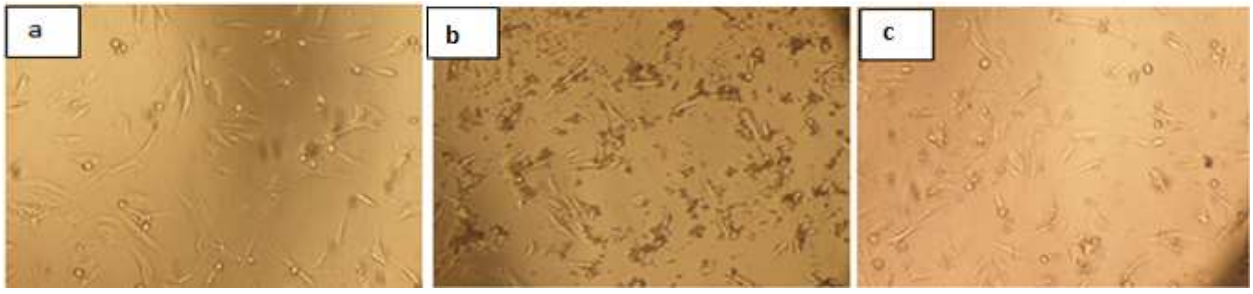

Figure 13: ADSCs cell proliferation in 24 hours a.TCP b. ZnO and c. MgO

The in-vitro cytotoxicity of all magnesium oxide and zinc oxide nanorods in both milligram and nanogram were observed using tissue culture plate as control .From the above data, it was observed that, more amount of sample induced cell proliferation leading to a conclusion that using of such samples for load bearing implants won't hinder but induce growth.

CONCLUSION

The study concludes, that when desiging composites for load bearing applictions, both mechanical strenght as well as cell behaviour has to be considered to avoid immune rejection and proper grafting of the biomimitic material for better bone tissue engineering.

REFERENCES

1. Green, D., et al., *The potential of biomimesis in bone tissue engineering: lessons from the design and synthesis of invertebrate skeletons.* Bone, 2002. **30**(6): p. 810-815.
2. Castaneda, C., *Muscle wasting and protein metabolism.* J Anim Sci, 2002. **80**(Suppl 2): p. E98-E105.
3. Zhang, L. and T.J. Webster, *Nanotechnology and nanomaterials: promises for improved tissue regeneration.* Nano Today, 2009. **4**(1): p. 66-80.
4. Burg, K.J., S. Porter, and J.F. Kellam, *Biomaterial developments for bone tissue engineering.* Biomaterials, 2000. **21**(23): p. 2347-2359.
5. Hollister, S.J., *Porous scaffold design for tissue engineering.* Nature materials, 2005. **4**(7): p. 518-524.
6. Lin, G., H. Zhang, and L. Huang, *Smart polymeric nanoparticles for cancer gene delivery.* Molecular pharmaceutics, 2014.
7. Bandyopadhyay-Ghosh, S., *Bone as a collagen-hydroxyapatite composite and its repair.* Trends Biomater Artif Organs, 2008. **22**(2): p. 116-124.
8. Rezwan, K., et al., *Biodegradable and bioactive porous polymer/inorganic composite scaffolds for bone tissue engineering.* Biomaterials, 2006. **27**(18): p. 3413-3431.
9. Kretlow, J.D. and A.G. Mikos, *Review: mineralization of synthetic polymer scaffolds for bone tissue engineering.* Tissue engineering, 2007. **13**(5): p. 927-938.
10. Luo, C., et al., *Electrospinning versus fibre production methods: from specifics to technological convergence.* Chemical Society Reviews, 2012. **41**(13): p. 4708-4735.
11. Heimann, R.B. and H.D. Lehmann, *Bioceramic Coatings for Medical Implants: Trends and Techniques*2015: John Wiley & Sons.
12. Zhou, H. and J. Lee, *Nanoscale hydroxyapatite particles for bone tissue engineering.* Acta Biomaterialia, 2011. **7**(7): p. 2769-2781.
13. Mravic, M., B. Péault, and A.W. James, *Current trends in bone tissue engineering.* BioMed research international, 2014. **2014**.
14. Khalil, H.A., A. Bhat, and A.I. Yusra, *Green composites from sustainable cellulose nanofibrils: A review.* Carbohydrate Polymers, 2012. **87**(2): p. 963-979.

15. Kumar, M.N.R., *A review of chitin and chitosan applications.* Reactive and functional polymers, 2000. **46**(1): p. 1-27.
16. Biarnés, X., et al., *The conformational free energy landscape of β-d-glucopyranose. Implications for substrate preactivation in β-glucoside hydrolases.* Journal of the American Chemical Society, 2007. **129**(35): p. 10686-10693.
17. George, S. and I. Goldberg, *Self-assembly of supramolecular porphyrin arrays by hydrogen bonding: new structures and reflections.* Crystal growth & design, 2006. **6**(3): p. 755-762.
18. Gandini, A., *Polymers from renewable resources: a challenge for the future of macromolecular materials.* Macromolecules, 2008. **41**(24): p. 9491-9504.
19. Crini, G., *Recent developments in polysaccharide-based materials used as adsorbents in wastewater treatment.* Progress in polymer science, 2005. **30**(1): p. 38-70.
20. Mohanty, A.K., M. Misra, and L.T. Drzal, *Natural fibers, biopolymers, and biocomposites*2005: CRC Press.
21. Lavoine, N., et al., *Microfibrillated cellulose–Its barrier properties and applications in cellulosic materials: A review.* Carbohydrate Polymers, 2012. **90**(2): p. 735-764.
22. Bondeson, D., A. Mathew, and K. Oksman, *Optimization of the isolation of nanocrystals from microcrystalline cellulose by acid hydrolysis.* Cellulose, 2006. **13**(2): p. 171-180.
23. Isogai, A. and Y. Kato, *Preparation of polyuronic acid from cellulose by TEMPO-mediated oxidation.* Cellulose, 1998. **5**(3): p. 153-164.
24. Habibi, Y., L.A. Lucia, and O.J. Rojas, *Cellulose nanocrystals: chemistry, self-assembly, and applications.* Chemical reviews, 2010. **110**(6): p. 3479-3500.
25. Kumar, A.P., et al., *Nanoscale particles for polymer degradation and stabilization—trends and future perspectives.* Progress in polymer science, 2009. **34**(6): p. 479-515.
26. Siqueira, G., J. Bras, and A. Dufresne, *Cellulosic bionanocomposites: a review of preparation, properties and applications.* Polymers, 2010. **2**(4): p. 728-765.
27. Kato, N. and S.H. Gehrke, *Microporous, fast response cellulose ether hydrogel prepared by freeze-drying.* Colloids and Surfaces B: Biointerfaces, 2004. **38**(3): p. 191-196.
28. Jiang, S., et al., *Tough and transparent nylon-6 electrospun nanofiber reinforced melamine–formaldehyde composites.* ACS applied materials & interfaces, 2012. **4**(5): p. 2597-2603.

29. Basu, S. and S. Ghose, *27—FUNGAL DECOMPOSITION OF JUTE FIBRE AND CELLULOSE: Part IV—The Action of Sòme Physical and Chemical Agencies on Subsequent Fungal Decomposition of Jute.* Journal of the Textile Institute Transactions, 1952. **43**(8): p. T355-T361.
30. Balagopalan, C., *Cassava utilization in food, feed and industry.* Cassava: Biology, production and utilization, 2002: p. 301-318.
31. Tuzlakoglu, K., et al., *Production and characterization of chitosan fibers and 3-D fiber mesh scaffolds for tissue engineering applications.* Macromolecular bioscience, 2004. **4**(8): p. 811-819.
32. Zhang, D., et al., *Consolidated pretreatment and hydrolysis of plant biomass expressing cell wall degrading enzymes.* BioEnergy Research, 2011. **4**(4): p. 276-286.
33. Shah, K., et al., *DECCAN PHARMA JOURNAL SERIES.*
34. Otshudi, A.L., A. Vercruysse, and A. Foriers, *Contribution to the ethnobotanical, phytochemical and pharmacological studies of traditionally used medicinal plants in the treatment of dysentery and diarrhoea in Lomela area, Democratic Republic of Congo (DRC).* Journal of ethnopharmacology, 2000. **71**(3): p. 411-423.
35. David, A.A., et al., *Anti-Vibrio and preliminary phytochemical characteristics of crude methanolic extracts of the leaves of Dialium guineense (Wild).* J. Med. Plants Res, 2011. **5**(11): p. 2398-2404.
36. Ordonez, A., J. Gomez, and M. Vattuone, *Antioxidant activities of Sechium edule (Jacq.) Swartz extracts.* Food chemistry, 2006. **97**(3): p. 452-458.
37. Albacarys, L.D., D.M. McAtee, and G.E. Deckner, *Disposable cleaning sheets with froths and surfactants*, 2002, Google Patents.
38. Ukpong, I., B. Abasiekong, and B. Etuk, *Phytochemical screening and mineral elements composition of Xanthosoma sagittifolium inflorescence.* Asian Journal of Plant Science and Research, 2014. **4**(6): p. 32-35.
39. Makin, O.S., et al., *Molecular basis for amyloid fibril formation and stability.* Proceedings of the National Academy of Sciences of the United States of America, 2005. **102**(2): p. 315-320.

40. Mano, J., et al., *Natural origin biodegradable systems in tissue engineering and regenerative medicine: present status and some moving trends.* Journal of the Royal Society Interface, 2007. **4**(17): p. 999-1030.
41. Klemm, D., et al., *Nanocelluloses: a new family of nature-based materials.* Angewandte Chemie International Edition, 2011. **50**(24): p. 5438-5466.
42. Pei, A., Q. Zhou, and L.A. Berglund, *Functionalized cellulose nanocrystals as biobased nucleation agents in poly (l-lactide)(PLLA)–crystallization and mechanical property effects.* Composites Science and Technology, 2010. **70**(5): p. 815-821.
43. Shyama Prasad Rao, R., *Studies on Water Extractable Feruloyl Polysaccharides from Native and Germinated Rice (Oryza Sativa) and Ragi (Eleusine Coracana)*, 2005, University of Mysore.
44. Carrillo, F., et al., *Structural FTIR analysis and thermal characterisation of lyocell and viscose-type fibres.* European Polymer Journal, 2004. **40**(9): p. 2229-2234.
45. Kilic, J.A., *Fungal decomposition dynamics using Fourier transform infrared spectroscopy and atomic force microscopy*, 2013, Rutgers University-Graduate School-New Brunswick.
46. Cuba-Chiem, L.T., et al., *In situ particle film ATR FTIR spectroscopy of carboxymethyl cellulose adsorption on talc: binding mechanism, pH effects, and adsorption kinetics.* Langmuir, 2008. **24**(15): p. 8036-8044.
47. Oksman, K., et al., *Manufacturing process of cellulose whiskers/polylactic acid nanocomposites.* Composites Science and Technology, 2006. **66**(15): p. 2776-2784.
48. Bras, J., et al., *Mechanical, barrier, and biodegradability properties of bagasse cellulose whiskers reinforced natural rubber nanocomposites.* Industrial Crops and Products, 2010. **32**(3): p. 627-633.
49. Srinivasan, C., et al., *Demonstration of Laccase in the White rot Basidiomycete Phanerochaete chrysosporium BKM-F1767.* Applied and Environmental Microbiology, 1995. **61**(12): p. 4274-4277.
50. Hakimi, O., et al., *Spider and mulberry silkworm silks as compatible biomaterials.* Composites Part B: Engineering, 2007. **38**(3): p. 324-337.

51. Lutolf, M. and J. Hubbell, *Synthetic biomaterials as instructive extracellular microenvironments for morphogenesis in tissue engineering.* Nature biotechnology, 2005. **23**(1): p. 47-55.
52. Kharlampieva, E., et al., *Co-cross-linking silk matrices with silica nanostructures for robust ultrathin nanocomposites.* ACS nano, 2010. **4**(12): p. 7053-7063.
53. Karageorgiou, V. and D. Kaplan, *Porosity of 3D biomaterial scaffolds and osteogenesis.* Biomaterials, 2005. **26**(27): p. 5474-5491.
54. Lewis, R.V., *Spider silk: ancient ideas for new biomaterials.* Chemical reviews, 2006. **106**(9): p. 3762-3774.
55. Grey, C., *Tissue Engineering Scaffold Fabrication and Processing Techniques to Improve Cellular Infiltration.* 2014.
56. Lepore, E., et al., *Silk reinforced with graphene or carbon nanotubes spun by spiders.* arXiv preprint arXiv:1504.06751, 2015.
57. Altman, G.H., et al., *Silk-based biomaterials.* Biomaterials, 2003. **24**(3): p. 401-416.
58. Eisoldt, L., A. Smith, and T. Scheibel, *Decoding the secrets of spider silk.* Materials Today, 2011. **14**(3): p. 80-86.
59. Ayoub, N.A., et al., *Blueprint for a high-performance biomaterial: full-length spider dragline silk genes.* PLoS One, 2007. **2**(6): p. e514.
60. Vollrath, F. and D.P. Knight, *Liquid crystalline spinning of spider silk.* Nature, 2001. **410**(6828): p. 541-548.
61. Ahmed, H., *Principles and reactions of protein extraction, purification, and characterization*2004: CRC Press.
62. Ray, A., et al., *Two Zn (II) and one Mn (II) complexes using two different hydrazone ligands: spectroscopic studies and structural aspects.* Structural Chemistry, 2008. **19**(2): p. 209-217.
63. Crini, G., *Non-conventional low-cost adsorbents for dye removal: a review.* Bioresource technology, 2006. **97**(9): p. 1061-1085.
64. Whitmore, L. and B. Wallace, *DICHROWEB, an online server for protein secondary structure analyses from circular dichroism spectroscopic data.* Nucleic acids research, 2004. **32**(suppl 2): p. W668-W673.

65. Day, L.A., *Circular dichroism and ultraviolet absorption of a deoxyribonucleic acid binding protein of filamentous bacteriophage.* Biochemistry, 1973. **12**(26): p. 5329-5339.
66. Mosekilde, L., *Age-related changes in bone mass, structure, and strength–effects of loading.* Zeitschrift für Rheumatologie, 2000. **59**(1): p. I1-I9.
67. Bauer, S., et al., *Engineering biocompatible implant surfaces: Part I: Materials and surfaces.* Progress in Materials Science, 2013. **58**(3): p. 261-326.
68. Anselme, K., *Osteoblast adhesion on biomaterials.* Biomaterials, 2000. **21**(7): p. 667-681.
69. Al-Hazmi, F., et al., *A new large–Scale synthesis of magnesium oxide nanowires: Structural and antibacterial properties.* Superlattices and Microstructures, 2012. **52**(2): p. 200-209.
70. Tormala, P., et al., *Layered surgical biocomposite material*, 1992, Google Patents.
71. Wilson, S.A., et al., *New materials for micro-scale sensors and actuators: An engineering review.* Materials Science and Engineering: R: Reports, 2007. **56**(1): p. 1-129.
72. Yu, J.C., et al., *Synthesis and characterization of porous magnesium hydroxide and oxide nanoplates.* The Journal of Physical Chemistry B, 2004. **108**(1): p. 64-70.
73. Yadav, T., et al., *Nanostructured fillers and carriers*, 2001, Google Patents.